



CZECH TECHNICAL  
UNIVERSITY  
IN PRAGUE

**F3**

**Faculty of Electrical Engineering  
Department of Measurement**

**Bachelor's Thesis**

# **On-board computer for PC104 format CubeSats**

**Filip Geib**

**Cybernetics and Robotics**

**May 2021**

**Supervisor: Ing. Vojtěch Petrucha, Ph.D.**



## **Acknowledgement / Declaration**

I would like to express my gratitude to VisionSpace Technologies, namely to José Feiteirinha, for conducting and sponsoring this project. I also thank my supervisor Vojtěch Petrucha for his guidance and support.

I hereby declare that the presented work was developed independently and that I have listed all sources of information used within it in accordance with the methodical instructions for observing the ethical principles in the preparation of university theses.

In Prague on May 21, 2021

.....

## Abstrakt / Abstract

**Klúčové slová:** CubeSat; FlatSat; OBC; PC104; radiačné testovanie.

**Preklad titulu:** Palubný počítač pre CubeSaty formátu PC104

This thesis is focused on the development of PC/104 format electronic boards for CubeSat applications. Particular attention was given to a single on-board computer (OBC) module. This universal ARM-based OBC is driven by an STM32L4 microcontroller supporting a great number of interfaces. Its additional features include robust power management, separate peripheral isolation, triple-redundant FLASH and F-RAM memories, dual CAN bus transceivers, inbuild temperature monitoring, and a significant payload sector. A dedicated radiation testing was conducted under a gamma radiation source. Moreover, three additional boards were developed, including a double redundant version of the OBC, a universal PC/104 module, and a FlatSat test bench. All of these boards were designed with open-source principles in a KiCad environment. This thesis contributes to the VisionSpace Technologies VST104 project by introducing a hardware platform for mission control systems testing and compression algorithms development.

**Keywords:** CubeSat; FlatSat; OBC; PC104; radiation testing.

# Contents /

<b>1 Introduction</b>	<b>1</b>
<b>2 VST104 project</b>	<b>2</b>
2.1 Project background . . . . .	2
2.1.1 CubeSat concept . . . . .	2
2.1.2 PC/104 standard . . . . .	3
2.1.3 Flatsat test bench . . . . .	4
2.1.4 On-Board Computer . . . . .	4
2.1.5 Existing OBC modules . . . .	4
2.2 Project motivation . . . . .	5
2.2.1 VST104 boards family . . . .	6
2.2.2 Community & open-source .	6
2.3 Project workflow . . . . .	7
2.3.1 KiCad and its plugins . . . .	7
2.3.2 VST104 KiCad libraries . . . .	8
2.3.3 GitHub repository . . . . .	8
2.3.4 Main header pinout . . . . .	8
2.3.5 PCB assembly . . . . .	9
<b>3 Board Sierra</b>	<b>10</b>
3.1 OBC characteristics . . . . .	10
3.1.1 Radiation and redundancy .	10
3.1.2 Capabilities and features .	11
3.1.3 Hardware architecture . . .	12
3.2 Electronic components . . . . .	12
3.2.1 Components certification .	12
3.2.2 Power consumption . . . . .	13
3.2.3 Additional parameters . . .	14
3.3 PCB features and design . . . .	14
3.3.1 PCB requirements . . . . .	14
3.3.2 OBC and payload sector .	15
3.3.3 PCB characteristics . . . .	15
3.3.4 Traces, vias and routing .	15
<b>4 Board Sierra - subsystems</b>	<b>17</b>
4.1 Microcontroller . . . . .	17
4.1.1 Schematic design . . . . .	18
4.1.2 PCB design . . . . .	18
4.2 External clock sources . . . . .	19
4.2.1 Schematic design . . . . .	20
4.2.2 PCB design . . . . .	20
4.3 Power management . . . . .	20
4.3.1 Schematic design . . . . .	21
4.3.2 PCB design . . . . .	22
4.4 Peripheral isolators . . . . .	23
4.4.1 Schematic design . . . . .	23
4.4.2 PCB design . . . . .	24
4.5 External memory . . . . .	25
4.5.1 Schematic design . . . . .	26
4.5.2 PCB design . . . . .	26
4.6 CAN bus drivers . . . . .	27
4.6.1 Schematic design . . . . .	27
4.6.2 PCB design . . . . .	28
4.7 Temperature monitoring . . . .	29
4.7.1 Schematic design . . . . .	29
4.7.2 PCB design . . . . .	30
4.8 Debug connector . . . . .	31
4.8.1 Schematic design . . . . .	32
4.8.2 PCB design . . . . .	33
4.9 Payload sector . . . . .	33
<b>5 Board Delta</b>	<b>34</b>
5.1 Motivation and expectation . .	34
5.2 Double redundant design . . .	35
5.2.1 Schematic design . . . . .	35
5.2.2 PCB design . . . . .	36
<b>6 Element Foxtrot</b>	<b>37</b>
6.1 FlatSat design . . . . .	37
6.2 Power supply features . . . .	37
6.3 Power supply circuitry . . . .	39
6.4 PCB design . . . . .	41
<b>7 Board Sierra - testing</b>	<b>42</b>
7.1 Testing software . . . . .	42
7.2 Radiation testing . . . . .	42
7.2.1 Experiment setup . . . . .	42
7.2.2 Experiment results . . . . .	44
7.2.3 Experiment summary . . .	47
<b>8 Conclusion</b>	<b>48</b>
<b>References</b>	<b>49</b>
<b>A Thesis assignment</b>	<b>53</b>
<b>B Glossary</b>	<b>54</b>
<b>C VST104 pinout</b>	<b>56</b>
<b>D Photo documentation</b>	<b>57</b>
<b>E Over-sized figures</b>	<b>61</b>
<b>F Additional materials</b>	<b>66</b>

# Tables / Figures

<b>3.1</b> Subsystems consumption .....	14	<b>2.1</b> Existing CubeSats .....	2
<b>4.1</b> Microcontroller parameters ....	18	<b>2.2</b> PC/104 board dimensions .....	3
<b>4.2</b> Power management rating .....	22	<b>2.3</b> PC/104 board dimensions .....	4
<b>4.3</b> External memory parameters..	26	<b>2.4</b> Existing OBCs and Flatsat .....	5
<b>4.4</b> Temp. sensors description .....	30	<b>3.1</b> Board Sierra 3D render .....	10
<b>8.1</b> VST104 pinout .....	56	<b>3.2</b> Sierra HW architecture .....	12
<b>8.2</b> Components consumption .....	66	<b>4.1</b> Sierra subsystems summary ...	17
<b>8.3</b> Uncertified parts variants.....	66	<b>4.2</b> Microcontroller circuitry .....	19
		<b>4.3</b> Clock sources schematic .....	20
		<b>4.4</b> Clock sources circuitry .....	21
		<b>4.5</b> Power management diagram...	21
		<b>4.6</b> Power management schematic .	22
		<b>4.7</b> Power management circuitry ..	23
		<b>4.8</b> Peripheral isolators diagram ...	24
		<b>4.9</b> Peripheral isolators schematic .	24
		<b>4.10</b> Peripheral isolators circuitry ..	25
		<b>4.11</b> External memory schematic ...	26
		<b>4.12</b> External memory circuitry.....	27
		<b>4.13</b> CAN drivers schematic .....	28
		<b>4.14</b> CAN drivers circuitry .....	28
		<b>4.15</b> Temp. monitoring schematic ..	30
		<b>4.16</b> Thermal bridge illustration ....	31
		<b>4.17</b> Temp. monitoring circuitry....	31
		<b>4.18</b> Debug connector pinout .....	32
		<b>4.19</b> Debug connector schematic ....	32
		<b>4.20</b> Debug connector circuitry .....	33
		<b>5.1</b> Board Delta 3D render .....	34
		<b>5.2</b> Board Delta KiCad .....	36
		<b>6.1</b> Foxtrot functionality .....	38
		<b>6.2</b> Foxtrot HW architecture .....	39
		<b>6.3</b> Foxtrot circuitry summary.....	41
		<b>7.1</b> Radiation: hardware setup ....	43
		<b>7.2</b> Radiation: OBC decay.....	44
		<b>7.3</b> Radiation: current consump... .	45
		<b>7.4</b> Radiation: OBC temperature .	45
		<b>7.5</b> Radiation: LSM6DS3 data ....	46
		<b>7.6</b> Radiation: MMC5983 data ....	46
		<b>7.7</b> Radiation: MPU6050 data.....	47
		<b>8.1</b> Thesis assignment .....	53
		<b>8.2</b> VST104 pinout .....	56
		<b>8.3</b> VST104 pinout .....	57
		<b>??</b> VST104 pinout .....	??
		<b>??</b> VST104 pinout .....	??
		<b>??</b> VST104 pinout .....	??
		<b>??</b> VST104 pinout .....	??
		<b>8.8</b> Board Zero render top .....	61

<b>8.9</b>	Board Sierra render top.....	62
<b>8.10</b>	Board Sierra render bottom ...	62
<b>8.11</b>	Microcontroller schematic .....	63
<b>8.12</b>	Element Foxtrot render .....	64
<b>8.13</b>	Element Foxtrot KiCad .....	65



# Chapter 1

## Introduction

An ongoing revolution in the space sector is known under the name of New Space. Innovative entrepreneurs are entering the field traditionally occupied by institutions to exploit new opportunities. One of the promising domains is the space data [1]. Precise navigation and planning, Earth environment monitoring, security and surveillance, internet of things communications. These are only a few examples of possible services that could be offered to various terrestrial companies and even the general public.

“Access to space is now broadening thanks to technology miniaturization. With a tremendous forecasted increase in the launch rate for small satellites, constellations are getting attention again from sustainable businesses.” [2] Although the small physical size of spacecrafts makes the space more affordable, it is also a very limiting factor in terms of those systems performance [1]. A possible solution could be the development of new algorithms and processing techniques tailored for these specific space applications.

VisionSpace Technologies (VST) is a New Space company located in the German city of Darmstadt, developing and integrating enterprise-level solutions for satellite missions. For some time now, the company has been working on algorithms for telemetry data compression and constellations mission planning. In 2020, the company decided to create a small hardware platform for testing mission control systems and the further development of the mentioned algorithms [3]. This platform was meant to consist of an open-source family of electronics boards in the Cubesat PC/104 format, including series of onboard computers and various development auxiliaries. The VST did not intend to create launchable products. Although complying with the nuances of space engineering was expected in order to develop a hardware with appropriate characteristics.

In the same year, we have joined the company as a summer intern to proceed with this hardware development project. In this thesis, we present our commitment to the project while providing documentation for the developed boards. Chapter two briefly introduces the related space background and the project’s motivation, goals, and workflow. Chapters three, four, and five are devoted to the developed Cubesat modules, describing the particular development steps and provide documentation for the modules’ designs. Chapter six presents the design of an auxiliary FlatSat test bench. The results of a radiation testing of one of the modules are shown in the last chapter.

## Chapter 2

### VST104 project

The project presented in this thesis is being conducted and sponsored by the company VisionSpace Technologies (VST). The project name, VST104, is a compilation of the company abbreviation VST and standard CubeSat board format PC/104 (described in section 2.1.2). In this chapter, we present a brief introduction into related space industry background together with the project's motivation, goals and workflow.

#### 2.1 Project background

The VST104 project is about designing electronics hardware for space applications. Therefore a fundamental orientation in a part of the space industry jargon is required. In this section, we provide a short introduction to the corresponding space industry concepts. We briefly explain what CubeSats, PC/104 boards, Fltsats, and onboard computers (OBCs) are. A summary of recently available OBC modules is also listed.

##### 2.1.1 CubeSat concept

CubeSats are modular spacecraft from a picosatellite class, usually constructed of similar components and limited to specific dimensions and materials. CubeSats are being developed in several sizes, which are based on a standard 1U unit [4]. This unit is defined as being  $100.0 \pm 0.1[\text{mm}]$  wide and  $113.5 \pm 0.1[\text{mm}]$  tall, with a limited mass of  $1.33[\text{kg}]$  [5]. Numerous CubeSats also include deployable subsystems, such as antennas, probes, or solar panels that exceed the normative dimensions when deployed [6]. For illustration, some of the already launched CubeSats are shown in figure 2.1.

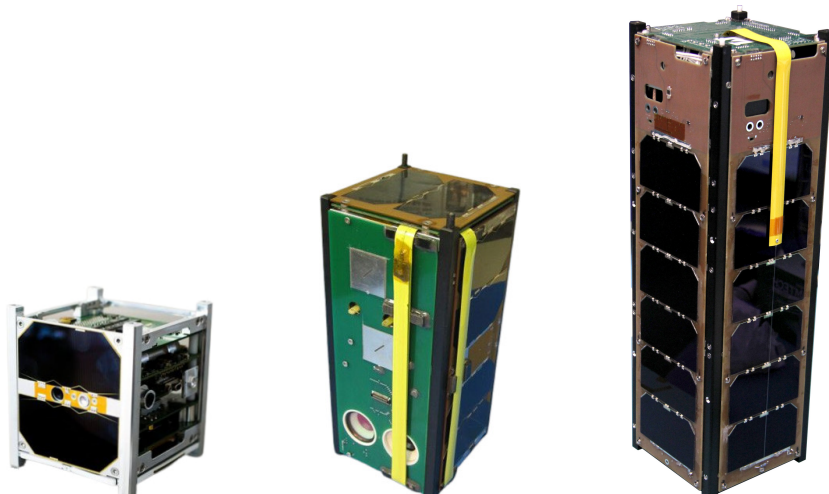


**Figure 2.1.** Photos of already launched CubeSats of various sizes. 1U SkCube (left), 2U Antelsat (center), 3U Grifex (right). Sources: TASR, GAUSS, NASA.

“CubeSats are very popular among universities and other non-commercial groups globally. Larger space companies are developing CubeSat missions in-house to train new employees and assess the possibilities of new technologies.” [7] “Several types of CubeSats have been developed and deployed for a specific mission, such as research and development satellites, earth remote sensing satellites, and space tethers satellites.” [8]

“A CubeSat must conform to specific criteria that control factors such as its shape, size, and weight. The standardized aspects of CubeSats make it possible for companies to mass-produce components and offer off-the-shelf parts. As a result, the engineering and development of CubeSats has become less costly than highly customized small satellites. The standardized shape and size reduces costs associated with transporting them to, and deploying into, space.” [4] Some of the standards were introduced by the concept’s originators in the CubeSat Design Specification [5]. A team from the JPL has compiled the CubeSat principles in The CubeSat Approach to Space Access [9].

## 2.1.2 PC/104 standard

“The CubeSat industry has adopted the PC/104 specifications [10] as a de-facto standard for electronic boards. Moreover, such specifications provide mechanical and electrical benefits towards CubeSat fabrication beyond the compatibility with different structure and electronics suppliers. Following the PC/104 specifications, all electronic boards must measure 90.17 x 95.89[mm], and the electric bus must allocate four rows with 26 contacts of standard 2.54[mm] spacing through-hole (THT) headers.” [11]

The PC/104 boards are meant to be stacked on top of each other, forming a rigid structure. The 104 pin headers provide a electrical connection between the individual boards, creating one electrical system. Excluding the headers, the PC/104 boards are firmly attached together with M3 standoffs placed in the corner mounting holes. This combination of the shared electrical bus and M3 bolts improves the stiffness provided by the CubeSat’s structure and simplifies the internal harnessing [11].

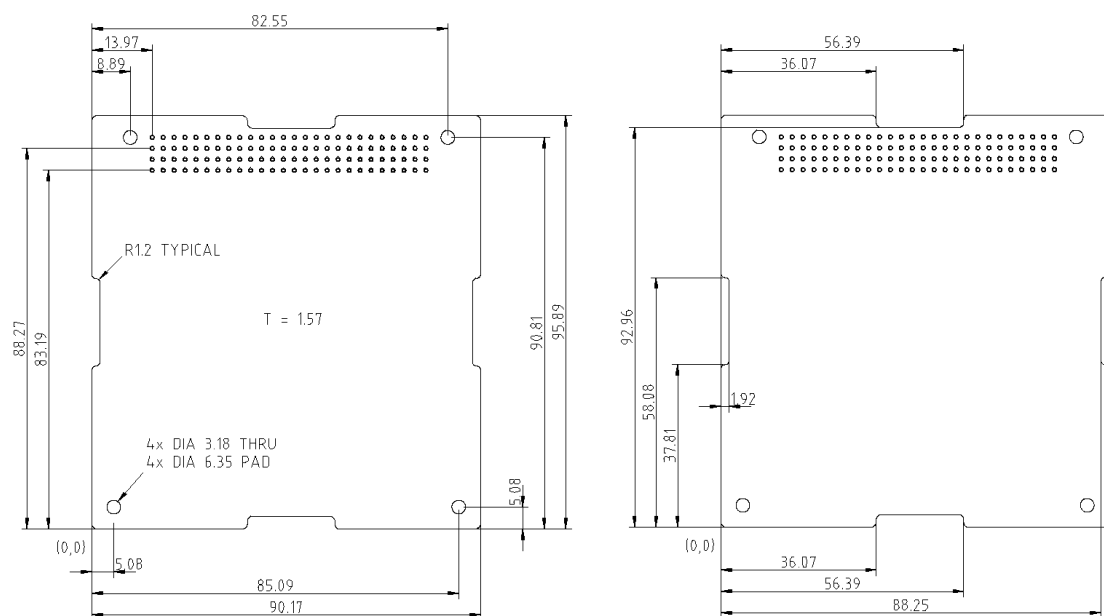


**Figure 2.2.** Technical drawings of the LibreCube PC/104 board. Overall geometry (left) and edge cutouts (right). All dimensions are in [mm]. Source: LibreCube.

As the PC/104 standard allows some freedom for changes, a slightly modified PC/104 board template was used in this project. The template was designed by the LibreCube initiative [12] and its drawings are shown in figure 2.2. The only modification done to the original PC/104 board are 1.9 x 20.3[mm] cutouts located on the board's four edges. These cutouts are designed to accommodate CubeSat's auxiliary cables.

### **2.1.3 Flatsat test bench**

During the hardware and software debugging and development, physical access to a particular CubeSat module is usually required. As the spacing between the stacked PC/104 boards is only 15.24[mm] [10], it is neither easy nor practical to work with these already stacked modules. Therefore, a test bench called Flatsat is often used to mount all of the CubeSats modules next to each other on a plain surface. This bench should substitute an electrical bus and connect all of the PC/104 headers together. Some of the available Flatsats accommodate additional features such as an inbuild power supply, sun power emulator, or ESD protection. A modular Flatsat is shown in figure 2.3.



**Figure 2.3.** The first version of the Aalto-3 Flatsat. Source: AaltoSatellites.

### **2.1.4 On-Board Computer**

“The onboard computer (OBC) in CubeSat is the module that acts as a bridge connecting the other modules with each other. It supervises many of the tasks done by the different modules of a satellite and performs housekeeping and monitoring to ensure the health and status of those modules. The hardware and software design of the OBC mainly depends on the mission of the CubeSat.” [13] The three main design parameters for OBC’s electronic subsystems are power consumption, physical dimensions, redundancy, and radiation environment behavior [14].

### **2.1.5 Existing OBC modules**

“Despite growing interest from industry in CubeSats as means of technology demonstration, such platforms are still primarily considered as an educational tool.” [11] Various universities and research institutions around the globe are developing and launching their own CubeSats. The failure rate of these university-build spacecrafts was estimated slightly below 50% in the first six months of their operation, as stated by two surveys from 2013 [15] and 2016 [16]. Since the OBC is a critical module and has caused 20% of these failures [16], it might be counterproductive to consider these designs as reference ones. Some of these CubeSats were although highly successful, and their OBC modules are worth mentioning. For example, the Atmel’s ARM based OBC of StudSat [17], or the 16-bit MSP430 microprocessor based OBCs of Libertad-1 [18] and RAX-2 [19].

A popular option for research institutions is to buy a professionally designed and already flight-proven CubeSat. Multiple space companies have therefore developed their own designs, including PC/104 OBC modules. Some of the recently available OBCs on the global market are: a rugged DP-OBC-0402 by Data Patterns [20], a high-performance iOBC by ISIS [21] (figure 2.4), state of the art IMT CubeSat OBC by IMT [22], a lightweight and cost-saving CubeSat OBC by German Orbital Systems [23], a motherboard for harsh environment CubeSat Kit Motherboard by Pumpkin [24], a general-purpose ABACUS by Gauss [25], an ‘always-on’ operation KRYTEN-M3 by AAC Clyde Space [26], a telemetry, tracking & command and data processing unit Antelope OBC by Antelope [27], a space-qualified processor unit NANOSATPRO by STM [28], an OBC for mission-critical space application NanoMind A712D by GomSpace [29] and a highly integrated main bus unit SatBus 3C2 by NanoAvionics [30] (figure 2.4). Regarding numerous successful flights and continuous development in a highly competitive industry, we can consider these OBCs as state-of-the-art designs. Multiple references to these modules can be found through the thesis.



**Figure 2.4.** Photos of existing professionally developed OBCs. iOBC by ISIS (left) and SatBus 3C2 by NanoAvionics (right). Sources: ISIS, NanoAvionics.

## 2.2 Project motivation

“Increasing the amount of science and housekeeping data increases a mission’s value, but this comes with extended costs and challenges, especially for CubeSat missions. The VST focuses on telemetry data compression, mainly the CCSDS standard ‘Robust compression of fixed-length housekeeping data’ (POCKET+) to tackle this problem. The algorithm performance was verified, and the VST developed a concept supporting multiple frame sizes.” [31] This includes the very first implementation of the POCKET+ in a hardware description language and synthesis for a radiation-hardened FPGA.

To enable the use and future development of this concept on CubeSats, the VST104 project was established by the company. The project’s main goal was set to develop a series of onboard computer (OBC) CubeSat modules serving as a software-defined platform. These boards should host a single or redundant OBC paired with an FPGA for hardware acceleration. It is essential to state that the VST104 project is still ongoing. Our contribution (thus the content of this thesis) was limited to developing early versions of the OBC modules and their auxiliaries. The motivation and expectation behind every one of them, together with the project’s open-source principles and contribution to CubeSat communities, are explained in the rest of this section.

## ■ 2.2.1 VST104 boards family

The family of boards developed under the VST104 project has four members at the time of writing this thesis. All of them were designed by ourselves as our contribution to this project. The role of each board in the project and its potential use cases are listed below. A detailed description of the boards is provided in the remaining chapters.

- **Board Zero:** A prototyping module in the PC/104 format. This board accommodates an array of THT pads with multiple 3.3[V], 5[V] and GND power rails, and four universal SO-24 footprints. The Board Zero should provide an efficient tool for rapid-prototyping temporary circuits with THT or SMD technology. Since the design of this board is very basic, no specific description is provided in this thesis. Nevertheless, the same design was implemented to a payload sector of the Board Sierra and is described in section 4.9. A 3D render of the Board Zero is shown in figure 8.8.
- **Board Sierra:** A single onboard compute (OBC) module in the PC/104 format. This board is the most important part of our contribution. The goal was to design a universal OBC while fulfilling most of the space industry requirements and keeping the manufacturing cost down [3]. This module should serve as a template for future VST140 OBC variants. Its significant payload sector is designed to be replaced with additional circuitry, particularly with an FPGA. The VST proposed development of this board to obtain a CubeSat computer module for future development and testing of various algorithms. Chapters 3 and 4 are fully devoted to this board.
- **Board Delta:** A double redundant PC/104 OBC module. “This board implements the Board Sierra in a double redundant configuration. The potential of this board is in user scenarios where reliability is essential. In case of system fraud, a supreme logic should simply switch between the identical OBCs sharing (almost) the same software and electrical characteristics.” [3] More details are provided in chapter 5.
- **Element Foxtrot:** A FlatSat test bench with an inbuilt power supply. This auxiliary board should serve as a development and show-off test bench, capable of hosting and powering up multiple PC/104 modules. “Element Foxtrot is an ideal tool for testing and developing different CubeSat modules, temporary replacement for power distribution unit (PDU), and a nice way to present already developed modules.” [3] Features and design of this FlatSat are fully described in chapter 6.

Future expansion of the VST104 board family is planned, and the VST team is currently working on new boards. The previously mentioned extension of the Board Sierra with an FPGA and its supporting circuitry should be the first one of them [31].

## ■ 2.2.2 Community & open-source

Concerning the previously explained motivation behind this project, there is no interest by the VST in developing their own CubeSat. However, some future software tests may require additional CubeSat systems. It should also be possible to easily integrate the VST104 modules into a third-party CubeSat during a flight opportunity. Therefore cooperation with existing organizations developing CubeSats is essential.

At the beginning of the project, some of the VST employees were already members of the LibreCube initiative. This organization aims to develop ready-for-use CubeSat elements for space and earth exploration missions. The VST supervisors decided to follow the LibreCube PC/104 template and their header pins assignment (as described in sections 2.1.2 and 2.3.4). This opened the possibility of combining the VST104 boards with any LibreCube element while contributing to such an exciting initiative.

Another organization that the VST supervisors chose to cooperate with is named TUDSaT. It is a research group formed by students at the local technical university of Darmstadt. These students are interested in space exploration, and one of their projects is developing a 1U CubeSat. Throughout our contribution to the VST104 family, we were in touch with their project leaders. We discussed some issues, and we both slightly tweaked our project for better compatibility. At the end of our internship, the TUDSaT received a fully assembled Board Sierra module together with an Element Foxtrot.

The VST supervisors intended the project to be fully open-source from its beginning. This decision was determined by multiple reasons. As the simultaneously developed VST software stack is free and open-source [31], proprietary hardware would make no sense. Being open-source is also required to be able to support and contribute to the two previously mentioned organizations. Both the LibreCube and TUDSaT share strong open-source philosophies. Lastly, the open-source concept goes hand in hand with CubeSats' educational and research principles. The entire VST104 project is licensed under the 'Strongly Reciprocal CERN Open Hardware Licence Version 2' (CERN-OHL-S) [32] and is publicly accessible on a company GitHub repository.

## 2.3 Project workflow

The VST104 project turned out to be quite complex, and we had to undergo multiple design steps. Many of them were related to a specific VST104 board, but some were more general. In this section, we address the design steps common for the entire project. We discuss the KiCad environment, the VST libraries, the project's GitHub repositories, the PC/104 pin assignment, and the assembly of the VST104 boards.

### 2.3.1 KiCad and its plugins

Since the VST104 project is mainly about designing electronics hardware, proper PCB design software had to be selected. There are multiple professional software packages available, such as Altium Designer or CadSoft EAGLE. Although these design tools come with powerful features, they do not fit with the open-source policy of the project (section 2.2.2). The VST supervisors chose the KiCad EDA instead. This tool is probably the most popular one in the open hardware and makers community. On top of that, both LibreCube and TUDSaT use KiCad for their projects.

As the KiCad is an open-source project itself, various extensions were created by the community. These action plugins are not included in the official KiCad distribution but are generally well-behaved and helpful. We have also used some of them during the development of the VST104 boards to compensate for missing features. Particularly:

- **Interactive HTML BOM<sup>1</sup>** for more convenient PCB assembly.
- **Teardrops<sup>2</sup>** to generate teardrop patterns for traces and pads.
- **Replicate layout<sup>3</sup>** to copy and paste chunks of traced circuitry.
- **RF-Tools for KiCAD<sup>4</sup>** to measure and tune differential pairs.

<sup>1</sup> <https://github.com/openscopoproject/InteractiveHtmlBom>

<sup>2</sup> [https://github.com/NilujePerchut/kicad\\_scripts/tree/master/teardrops](https://github.com/NilujePerchut/kicad_scripts/tree/master/teardrops)

<sup>3</sup> [https://github.com/MitjaNemec/Kicad\\_action\\_plugins/tree/master/replicate\\_layout](https://github.com/MitjaNemec/Kicad_action_plugins/tree/master/replicate_layout)

<sup>4</sup> <https://github.com/easyw/RF-tools-KiCAD>

### **2.3.2 VST104 KiCad libraries**

Although the KiCad official symbol libraries are pretty large, they do not include some of the electronic components used in the VST104 boards. The majority of these missing symbols correspond to specialized integrated circuits (ICs). To resolve this problem, we created a project-related symbol library containing all of the missing symbols. We designed these symbols accordingly to components' datasheets and the KiCad library conventions [33]. If a symbol was available in the official library, we have used it.

Every electronic component needs to be properly attached to the PCB's surface. An arrangement of pads required to solder the component on the PCB is called a footprint. Components with different standardized packages require corresponding footprints. These footprints are usually available for download on various websites or are included in the KiCad official libraries. Although it is comfortable to use these pre-made footprints, this approach brings inconsistency and dependency to the PCB design. Therefore we decided to create each of the used footprints by ourselves, following reference designs in components' datasheets and the KiCad library conventions [33].

It is a common feature in modern PCB design software such as KiCad to support a 3D visualization. Besides pads, copper traces, or drill holes, the 3D render can visualize particular electronic components. We consider this tool crucial for creating documentation or presenting the VST104 project. However, to enable this feature, WRL or STEP files containing the components' 3D models are required. Thus, while creating an individual component's footprint, we also searched the web for its 3D model files. The WRL provides support for material properties, allowing superior 3D rendering. Unfortunately, it is not so common for component manufacturers to offer this type of model. In such a case, a fake WRL was created from the available STEP file.

The **VST104-Libraries** are structured into three separate folders: **VST104\_symbols**, **VST104\_footprints**, and **VST104\_logos**. At the time of writing this thesis, the **VST104\_symbols** contain 16 symbols. The total number of 84 individual footprints and their associated WRL and STEP 3D models are included in the **VST\_footprints**. The **VST104\_logos** was not described in this section by now. This folder contains 14 silkscreen graphics of various logos in different sizes (VST, open-source Hardware, and LibreCube logo). These logos are used through all of the VST104 boards.

### **2.3.3 GitHub repository**

The entire VST104 project is available on the company's GitHub. The main repository is called **VST104<sup>5</sup>** and acts as a project crossroad. It lists connections to other repositories and provides a brief description of the project itself. Each of the VST104 boards has its own repository. This GitHub structure was suggested by the LibreCube community. Its main benefit is the possibility to push and review changes to the different boards separately. The VST libraries also have their separate GitHub repository linked as a submodule to each of the boards. With this approach, only one shared library exists instead of multiple board-limited libraries with duplicity content.

### **2.3.4 Main header pinout**

Despite the international effort to achieve modularity of the CubeSats, the pinout of the main PC/104 header changes between different manufacturers and missions. "The allocation and distribution topology for power are not taken over, nor standardized for CubeSats, leading to compatibility issues. Therefore, when PC/104 is mentioned as

---

<sup>5</sup> <https://github.com/visionspacetec/VST104>

standard in relation to CubeSats, this refers to a fixed physical wiring harness and the mechanical layout, and not the data bus or pin allocation.” [34] Therefore, as our first contribution to the VST104 project, we had to come with a reasonable pin assignment.

After researching publicly available pinouts of different CubeSat manufacturers and related organizations (NanoAvionics, ISIS, Gomspace, Endurosta, TUDSaT, LibreCubeSat, etc.) we proposed and implemented PC/104 pin assignment as shown in figure 8.2. Some of the signals with not so self-explaining names are explained in table 8.1. This so-called VTS pinout is present in all of the VST104 boards. Our main goal during its creation was to provide the highest compatibility with other CubeSats as possible while accommodating various data buses and system maintenance signals.

It is essential to state that the currently presented VTS pinout is a subject of change in the nearest future. Our presentation of the VST104 project at the Open Source CubeSat Workshop 2020 [3] started a discussion about the PC/104 header pin assignment. As a follow-up to this workshop, multiple online meetings regarding the pinout hold place. Organizations developing open-source CubeSats modules, such as VTS, LibreCube, AcubeSAT, or SatNOGS, are currently consolidating their pin assignments in order to become more compatible and possibly even uniformed.

### **2.3.5 PCB assembly**

A manual assembly of an electronics board is a time-consuming and, therefore, costly operation. This applies especially to double-sided boards with as many fine-pitch components as the Board Sierra and Delta have. To address this problem, we designed all VST104 boards accordingly to PCB industry requirements so that the boards can be populated with electronics components by an assembly machine. The required design properties were, for example, respecting the minimal fabrication clearance of a component or strictly following the suggested solder paste distribution areas. We also addressed these requirements during the previously mentioned creation of VST footprints (described in section 2.3.2) while creating the documentation, courtyard, and paste layers (named as `.Fab`, `.CrtYd`, `.Paste` in the KiCad jargon).

Exported Gerber files containing all of the fabrication and documentation layers are available for the VST104 boards in their GitHub repositories. Multiple versions of the bill of materials (BOM) files are also available for each board. This includes files generated with i) a standard KiCad BOM export, ii) the Interactive HTML BOM plugin (described in section 2.3.1), and iii) a project list on Mouser Electronics.

Despite the mentioned possibility of an automated assembly, we have manually populated a couple of the boards by ourselves. As the service of machine assembly is worthy only for higher quantities, it was not suitable for our development and testing purposes. By the end of the internship, we assembled four Board Sierra modules, together with four Element Foxtrot flatsats. Our approach can be summarized in the following steps: i) spread a solder paste to one side of the PCB using a stencil sheet, ii) place all of the electronics components to the PCB with the help of an optical microscope and precise tweezers, iii) preheat the PCB and sequentially solder the components with a hot air soldering station, iv) repeat the process with the other side of the board (if any). This method, especially step number ii, was tricky due to a small size of the components (most of the Board Sierra resistors footprints are 0201). However, all of the assembled boards turned out good and passed a visual and electrical inspection. Photographs of the assembled VST104 boards are listed in figures 100, 200, and 300.

# Chapter 3

## Board Sierra

This chapter addresses the design process and overall characteristics of the Board Sierra - a single OBC module in the PC/104 format. Design challenges, development decisions, and final features are explained in detail. Particular attention is given to the onboard computer, from now referred to as the OBC. A 3D visualization of the Board Sierra is shown in figure 3.1. A description of its subsystems is provided in chapter 4.

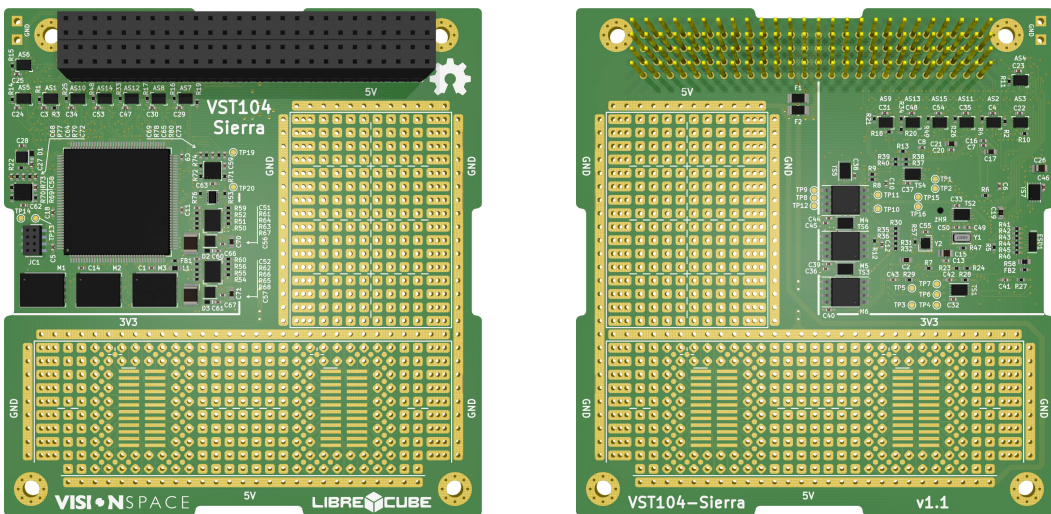


**Figure 3.1.** 3D render of the Board Sierra from the top (left) and the bottom side (right). A real scaled version of this visualization is available in figures 8.9 and 8.10.

### 3.1 OBC characteristics

An OBC of a CubeSat is a complex subsystem combining various features. Reviewing technical documentation of already existing OBCs (section 2.1.5) showed that some features are shared among most OBCs, whereas some are unique. In this section, we list all of the features we decided to implement, both typical and VST104 related.

#### 3.1.1 Radiation and redundancy

Occasionally traveling through weaker parts of the Earth's magnetic field and not shielded by the Earth's atmosphere, the CubeSats have to operate in an environment full of radiation. A direct hit of a high-energy particle might have serious consequences for OBC functionality. These include transistor gate ruptures, memory bit flips, software upsets, or latch-ups [35–37]. “Single event latch-ups and upsets can occur even in a low radiation environment like a polar LEO orbit.” [9] Proper measures have to be taken to increase the OBC durability and ability to handle errors, resulting in maximizing a mission lifetime. This process is known as radiation hardening (its results are labeled as *rad-hard* or *radiation-hardened*) and can be achieved by two different techniques.

A physical approach, also known as a radiation hardening by design, relies on special radiation-hardened components. Hardened ICs are manufactured on insulating substrates (rather than typical semiconductor wafers) or use some of the many dedicated design principles [35]. Implementation of this strategy is typical for professional and more expensive satellites than the CubeSats. These components are usually bigger, costly, and have reduced performance and functionality compared to ordinary ones.

Considering the size and budget requirements of our OBC, we chose to implement another option. Instead of the previously mentioned physical hardening technique, a logical one was realized. The OBC hosts multiple schematic design features ensuring the proper handling of any radiation-related event. These include: i) over-current sensing power management, ii) separate peripheral isolators, iii) full high-impedance mode requested by the higher logic, iv) triple-redundant memories, or v) multiple onboard temperature sensors. A fully double-redundant OBC is presented in chapter 5.

### **3.1.2 Capabilities and features**

Having in mind the expectations of the VST supervisors, features common for OBCs by different manufacturers (section 2.1.5), and design requirements implied by the radiation (section 3.1.1), we set and implemented the following OBC's features:

- **Microcontroller:** An ultra-low-power STM32L496 ARM Cortex-M4 core microcontroller drives the OBC. This MCU can run up to 78[MHz], is equipped with a 1[MB] flash memory and 320[kB] RAM, and provides a wide external connectivity. A user can program and debug this MCU using a separate SWI or UART connection.
- **External clock sources:** The MCU is equipped with two external clock sources for improved and more reliable clock generation and timing. Low-speed external 32.768[kHz] oscillator and high-speed external 26[MHz] oscillator. This oscillator can be temporarily disabled by the MCU to achieve better power consumption.
- **Robust power management:** Two separate power lines with 3.3[V] and 5[V] ratings supply the OBC. A robust power management circuitry is present separately on these lines, providing tunable over and under-voltage protection, over-current protection, amplified current monitoring output, kill switching, and simultaneous power down.
- **Isolation of the peripherals:** The OBC can communicate with other CubeSat modules using a 2x CAN bus, 3x I<sup>2</sup>C, 4x UART, 2x SPI, 22 GPIO pins, and 5 maintenance signals. All the peripherals are 5[V] tolerant and connected to the PC/104 header thru separate analog switches. These isolators are independently controlled by the MCU and provide a complete or selected disconnection from the rest of the CubeSat.
- **Redundant external memory:** Two subsystems of triple redundant external memories are available for MCU's additional data storage. This triple redundancy ensures data validity in the radiation-rich environment, although the single-mode is also supported. The first memory subsystem is a 3x 32[MB] FLASH connected via the Quad-SPI interface, while the second one is a 3x 2[Mb] F-ram using the SPI.
- **CAN bus peripherals:** Two CAN transceivers provide the OBC's support of a high-speed CAN bus. These transceivers ensure a voltage level conversion (3.3[V] for the MCU, 5[V] for the CubeSat) and support communication speeds up to 250[kB s<sup>-1</sup>].
- **Temperature monitoring:** Seven I<sup>2</sup>C temperature sensors are spread over the entire OBC. These sensors monitor the temperature of essential submodules, 2x MCU, 2x power management, 2x CAN bus drivers, and 1x external memories. The MCU can power on or off these sensors to save some power or resolve a latch-up even.
- **Maximal payload sector:** The PCB surface occupied by the OBC circuitry is shrank to the minimal size possible. The remaining area is considered as a payload sector

that can accommodate any user-defined modules. In our case, we decided to place a universal soldering array with exposed power lines all over this sector.

### 3.1.3 Hardware architecture

In the rest of this thesis, we address each of the previously mentioned features as a separate OBC subsystem. A diagram of the OBC hardware architecture is shown in figure 3.2. This diagram shows relations and used communication busses between all of the subsystems. For their detailed description, refer to the following chapter 4.

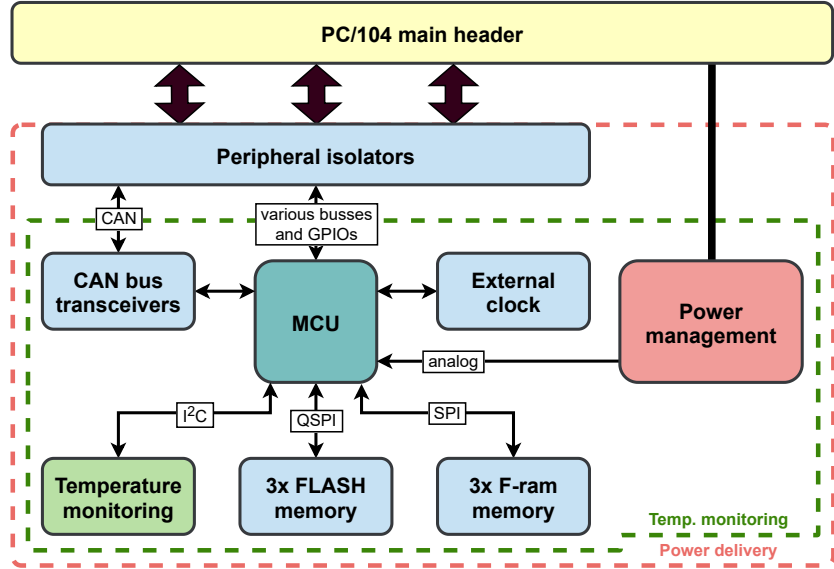


**Figure 3.2.** Diagram of the Board Sierra’s OBC hardware architecture.

## 3.2 Electronic components

Electronic components are the building stones of each electronic hardware. Big commercial, military, or research space crafts use specialized components designed, modified, or particularly selected for space applications. CubeSats, on the other hand, use in most cases commercial off-the-shelf (COTS) components that are not specifically designed for application within the space environment [6]. “The use of COTS components is certainly an attractive option for the development team of small satellite projects. Lead times are short, and recent developments in personal computing equipment and consumer electronic allow for high performance.” [7] Furthermore, these components have proven their low risk to mission success [9]. In the VST104 project, we have also decided to follow this trend and to use COTS components. In this section, we describe various requirements applied to these components and the criteria of their selection.

### 3.2.1 Components certification

Spacecrafts are exposed to a harsh environment and its effects during their lifetime. This problem also needs to be addressed on the electronic components level by selecting components with adequate parameters. The two essential criteria that need to be watched are operational temperature range and mechanical stress resistance.

“The temperature range that electronic components can encounter in orbit is quite large as the thermal control options are limited” [7]. “The most crucial impact on the

temperatures of a spacecraft is caused by the external radiation from Sun and Earth, as well as internal heat dissipation throughout electronic devices” [6]. Typical operational temperature for CubeSat components is in the range of  $-40$  to  $+85[^\circ\text{C}]$  [6–7], usually referred to as an industrial temperature range. As we wanted to be on the safe side, we decided to add a safety margin by extending the range. We chose the automotive range of  $-40$  to  $+125[^\circ\text{C}]$  as a requirement for electronic components in our design.

“During the launch, a spacecraft is subjected to various external loads resulting from vibroacoustic noise, booster ignition and burn out, propulsion system engine vibration, steady-state booster acceleration, and much more” [8]. Hence, various measures are applied to increase the robustness of the spacecraft. Regarding the OBC design, it was necessary to select only the electronic components meeting the AEC-Q100 and AEC-Q200 standards. “Components meeting these specifications are suitable for the harsh automotive environment without additional component-level qualification testing” [38].

To sum it up, all of the electronic components used in the Sierra Board i) are rated for the automotive temperature range of  $-40$  to  $+125[^\circ\text{C}]$ , and ii) obtained the AEC-Q100 or AEC-Q200 qualification. The only exception is the MCU with no AEC qualification.

Some of the OBC’s potential applications may not require temperature and automotive certification of the electronics components. In such a case, some components may be replaced by their uncertified variants to save a bit of the financial budget. All of the electronics components with an official uncertified version are listed in table 8.3. Furthermore, the potential user is encouraged to replace all passive components (resistors, capacitors, ferrite beads, inductors) with unqualified parts with the same parameters. A replacement of oscillators Y[1,2] is possible, although this change is non-negligible.

### **3.2.2 Power consumption**

CubeSat’s power budget is a closely monitored thing. Such a small spacecraft has a limited means of generating and storing electric power. Solar arrays are usually bound in their active surface and lack advanced tools of positioning. Similarly, battery storage systems are restricted by the available space and means of temperature control. It is crucial to minimize the power requirements of the CubeSat, including the OBC.

Reasonable power consumption of the OBC can be achieved on the level of electronic components selection by prioritizing the low-power components. A downfall of this approach is usually an implied decrease in their performance, speed, or frequency. Therefore, we preferred components with similar parameters but lower power consumption. This affected mostly the selection process in cases of the MCU and memory ICs.

Not only a component’s power consumption but also its efficiency is an important parameter. While choosing switching components such as electronic fuses, hot-side switches, or analog switches, a low on-resistance was preferred. Power losses on pull-down/pull-up resistors had to be also taken into consideration. A single  $10[\text{k}\Omega]$  pull-down resistor connected to a  $3.3[\text{V}]$  signal drains a constant current of  $330[\mu\text{A}]$ , creating a power loss of approximately  $1.1[\text{mW}]$ . During the schematic design, we aimed more at a subsystem’s robustness rather than avoiding this particular type of power loss. Therefore, some of the pull-down/pull-up resistors may be left unpopulated and their functionality compensated by programmable resistors integrated inside the MCU.

The summary of power consumption of the specific electronics components is listed in table 8.2. Overall power consumption of specific OBC’s submodules is listed in table 3.1. It sums power consumptions of all ICs and losses on pull-down/pull-up resistors in the particular subsystem. For the computation, two assumptions were made: i) full functionality of the subsystem, ii) input voltage range as described in table 4.2.

OBC subsystem	Typ. current [mA]	Note
Processing unit	20 @ 3.3[V]	at 80[MHz] clock
Power management	0.3 @ - [V]	for each 3.3[V] and 5[V] bus
Header isolation	0.6 @ 3.3[V]	every isolator is opened
FLASH memories	30 @ 3.3[V]	with one active memory
F-ram memories	5 @ 3.3[V]	with one active memory
Dual CAN bus	40 @ 5[V]	for each active CAN bus
Temp. monitoring	1.6 @ 3.3[V]	as a whole group

**Table 3.1.** A rough estimation of subsystems' power consumption during a normal operation at room temperature. This table should be used for orientation purposes only. A potential user is encouraged to conduct a proper measurement for each OBC application.

### 3.2.3 Additional parameters

A selection of particular electronic components is a vital part of designing circuitry. Usually, various electronic components share the same functionality and are available from different manufacturers. After filtering the available components by specific functionality (with respect to 3.2.1 and 3.2.2), it was common to find various suitable candidates. Therefore, additional criteriums had to be set to resolve the selection:

- **Price:** As this OBC is not primarily designed for an actual space flight (as explained in section 1), an individual component's price is not negligible. With a lower overall cost of the OBC, a broader project expansion in the LibreCube community can be achieved. Thus components with sufficient attributes but lower price were favored.
- **Footprint:** As a result of maximizing the PC/104 payload sector, the actual OBC area was significantly decreased. Therefore components of smaller dimensions available in fine-pitch packages (e.g. SSOP or QFN) were preferred. The same logic applies to passive components such as resistors and capacitors, resulting in a 0201 package (0603 in metric) being the most widely used in this design. After researching the technical capabilities and related costs of PCB manufacturers, we decided not to use the BGA-packaged components. Their significantly smaller footprints would require more precise fanout, resulting in increased manufacturing difficulty and price.
- **Distributor:** We considered it important to use only typically stocked components available from the global distributors. In our case, Mouser electronic<sup>1</sup>. This rule should repeal any future problems in components sourcing or logistics. Therefore, the availability of a specific component in this distributor was a selection factor.

## 3.3 PCB features and design

Designing the Board Sierra's PCB was probably the most demanding part of the VST104 project. Restricted surface available for the complex OBC's circuitry, compact footprint of the PC/104 main header with a not ideal location, and limited capabilities of the considered PCBs manufacturers made the routing and fanout challenging. Visualization of the designed module is shown in figures 8.9 and 8.10.

### 3.3.1 PCB requirements

The benefit of the Board Sierra's lower price regarding the particular electronic components was described in section 3.2.3. The same logic applies to the decision-making

<sup>1</sup> <http://www.mouser.com/>

during the PCB design. It is a common feature between PCBs manufacturers that the less advanced design, the cheaper PCB. This includes many parameters such as copper layer count, presence of buried vias and their size, copper clearances, tracks widths, and much more. On the other hand, fine features such as buried vias simplify the process of PCB design and allow more compact layouts. Therefore, it was crucial to find a balance between the manufacturing price and complexity of the OBC's layout and routing.

Although, following the proper design rules and standards created for automotive and especially space applications is much more important than lowering the PCB's manufacturing price. We addressed various requirements and suggestions listed in ECSS standards ECSS-Q-ST-70-12C [39] and ECSS-Q-ST-70-60C [40]. Other precious recommendations were found and implemented from the TEC-ED IoD Board Specification [41]. These specifications refer, for example, to track width and spacing, pad design, copper planes, or thermal rules. However, these documents are aimed at state-of-the-art spacecrafts designed and operated by the ESA. Thus a punctual following of all of the requirements and suggestions was not necessary for our CubeSat application.

### **3.3.2 OBC and payload sector**

As mentioned in section 3.1.2, a high ratio between the payload sector area and OBC area was set as one of the Board Sierra's key features. This requirement substantially affected the OBC's circuitry layout and fanout. After multiple iterations of components' placements and alignments, we have significantly reduced the required OBC area. The payload sector covers roughly three-fourths of the available PC/104 module surface, leaving only one-fourth to accommodate the OBC. Visual perception can be obtained from the Board Sierra 3D renders in figures 8.9 and 8.10. The OBC sector is situated at the northwest quartal of the PC/104 module, surrounded by the payload sector.

### **3.3.3 PCB characteristics**

The PCB's dimensions, geometry, and layout of the main connector and mounting holes are fully specified by the PC/104 standard, as described in section 2.1.2. The only modification added to this template are 1.9 x 20.3[mm] cutouts on the module's four edges. These cutouts were introduced in the LibreCube board specification and are designed to accommodate CubeSat's auxiliary power and data cables [12].

Regarding the manufacturing price and complexity, the PCB would ideally be a four-layer one. This means two copper layers for signal traces, a power distribution layer, and a ground plane. Unfortunately, the two signal layers would not be enough to accommodate complex OBC's circuitry. Therefore, we had to choose a six-layer PCB with the following setup: i) signal layers: top, second inner, bottom; ii) ground plane layers: first inner, fourth inner; iii) power distribution layers: third inner. "An additional benefit of the added layers is improved thermal dissipation, as adding a layer of copper to the circuit board can significantly decrease the resulting temperatures" [6].

Additional parameters of the PCB manufacturing such as material, isolation and copper thickness, surface finish and solder mask types are not specified in this thesis nor the VST104 project. It is the responsibility of the potential user to customize these parameters accordingly to the requirements of the specific application. In such a case, we encourage the user to follow relevant sections of the ECCS standard [39].

### **3.3.4 Traces, vias and routing**

Electronic components are placed on both sides of the PCB due to the restricted OBC area. Corresponding top and bottom copper layers cover as much routing as possible.

The second inside layer accommodates traces that do not fit into the two surface layers. The general width of a signal trace is 0.2[mm], respectively 0.173[mm] for traces near the PC/104 header. Clearance between traces themselves and other copper planes is set to 0.127[mm]. All of these parameters satisfy the minimal specifications in the ECSS standard [39]. No blind, buried or micro vias are used in the design. The diameter of general via is 0.45[mm] with a 0.24[mm] drill. These parameters result in a 6.7 aspect ratio for a standard 1.6[mm] thick PCB, which recognizes the ECSS  $\leq 7$  rule [39].

The first and fourth inner layers are ground plane layers. Their purpose is to connect all of the component's GND pins, provide shielding against the EMI and act as heatsink dissipating components heat. Despite the ECSS suggestion, both the ground planes have a solid fill instead of additional openings in a grid format [39]. The reason is, the current fifth version of KiCad does not support this option. This design flaw will be improved shortly as the checked fill option is included in the upcoming KiCad v6.

A copper plane with a solid fill is also located in the third inside layer. This plane is attached to a 3.3[V] power source, and its task is to connect all required components to this power bus. This layer also accommodates a 5[V] power distribution routing. Its traces are 0.45[mm] wide with multiple vias to minimize the potential voltage drop.

The final PCB routing highlighted by the particular OBC's subsystems is shown throughout multiple figures in chapter 4. General principles of good routing were implemented throughout the PCB design. These include steep turns avoiding, differential pairs matching, or sliver and peelable prevention [40]. If available, fanout and routing suggestions included in electronic components datasheets were followed. As suggested by the ECSS [39], a teardrop finish was applied to all of the pads using the KiCad Teardrops extension listed in section 2.2.2. It is important to mention that the current KiCad v5 does not support advanced design settings common for professional software such as Altium Designer or CadSoft EAGLE. Our approach to handling this problem was adding extra margins to the few parameters listed in KiCad, which increased the overall tolerance. The final PCB design passed a design rule check (DRC) with various parameters set according to manufacturers' standards and ECSS suggestions [40].

## Chapter 4

### Board Sierra - subsystems

In this chapter, we provide all details about the individual OBC subsystems. We address one of them in each section. Firstly, we explain the importance of the subsystem in theory, and then we describe our approach and the design decisions we made. We also present and comment on each subsystem's electronics scheme design together with the design of its layout and routing on the Board Sierra PCB. For a better image of the overall location and layout of these OBC subsystems, refer to figure 4.1.

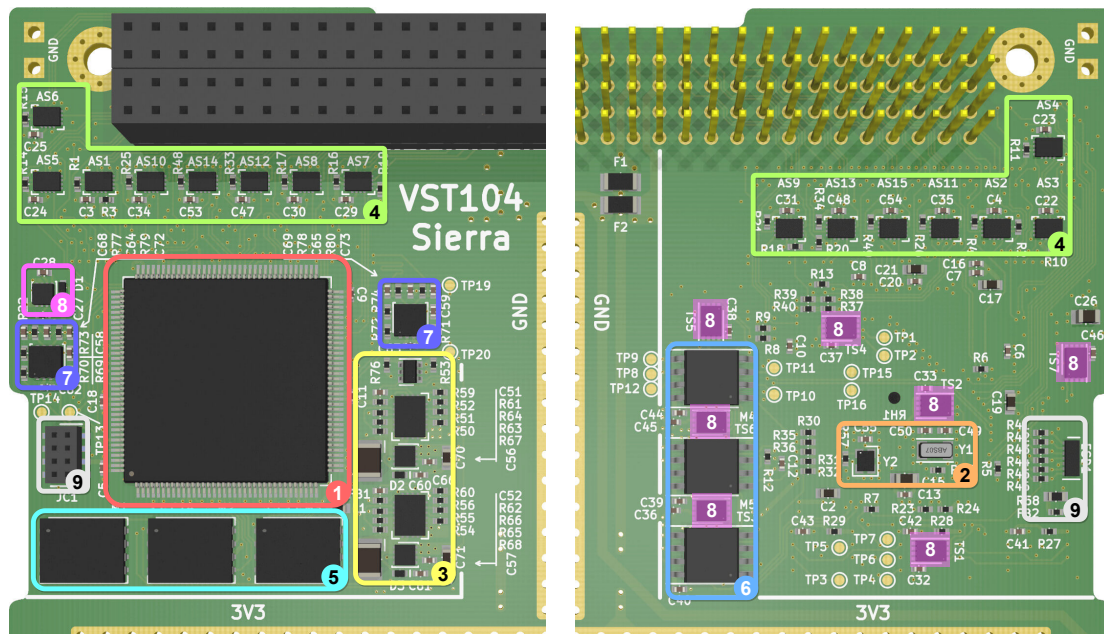


**Figure 4.1.** Location and layout of the Board Sierra OBC subsystems. The top side of the OBC is displayed on the left, whereas the bottom side is on the right. Legend: ① microcontroller, ② external clock sources, ③ power management, ④ peripheral isolators, ⑤ triple-redundant FLASH memory, ⑥ triple-redundant F-ram memory, ⑦ CAN bus transceivers, ⑧ onboard temperature sensors, and ⑨ SWD connector and circuitry.

#### 4.1 Microcontroller

The processing unit is the most important part of the OBC. Professional designs use MCUs with a wide variety of instruction set architectures [20, 22, 24–25, 28]. However, the ARM architecture seems to be the most popular [21, 23, 26–27, 29–30]. This architecture is known for its good multiprocessing support, low power consumption, affordable pricing, and existing applications in various fields. Considering these benefits and influenced by the LibreCube initiative, existing TUDSaT's project, and most importantly the VST supervisors, we decided to pick an STM32 microprocessor.

Our task was to choose a particular model of this 32-bit, Arm and Cortex-M based MCU. Aiming rather for a low-power than high-performance characteristics, we decided to select an L series. Particularly the L4 series as it combines the largest flash memory size with the highest number of general-purpose input/output pins (GPIOs) [42]. Although, only one device from the L4 series is equipped with two CAN bus channels. As the presence of a second bus is crucial for our double-redundant approach, the STM32L496xx option was selected. This family comes in six different packages. Avoiding all of the BGA-like ones (as described in section 3.2.3) narrows the selection to Zx, Vx, and Rx variants. The Zx is the most capable one in terms of flash size and GPIO count. Therefore the STM32L496ZG (where G stands for extended operating temperature range) was our final choice [43]. From now on, we will refer to this particular device as the MCU. Some of its key characteristics are listed in table 4.1.

Max. frequency	80 [MHz]	SPI	3
Flash memory	1 [MB]	I <sup>2</sup> C	4
Static RAM	320 [kB]	UART	5
Comparators	2	CAN	2
Op. amplifiers	2	GPIO	115
Operation temp.	−40 to 125 [°C]	DAC	2

**Table 4.1.** Highlighted characteristics of the STM32L469ZG microcontroller [43].

### ■ 4.1.1 Schematic design

The MCU pin assignment was continuously changing during the entire process of OBC schematic and PCB design. Its final state is presented in figure 8.11. We attempted to maximize the number of user-free GPIOs with added functionalities such as ADC or PWM while keeping the fanout manageable. A significant help during this process was the CubeMX tool of the STM32CubeIde, visualizing all of the pinout combinations with a specific functionality. Each of the 3.3[V] tolerant pins was used only for the internal circuitry, resulting in a fully 5[V] tolerant main PC104 header connection.

A significant number of filtering and reservoir capacitors is needed to ensure the proper MCU functionality. The assignment of correct capacitors to required MCU pins was pretty straightforward, following the device datasheet [43] and STM32L4 hardware development application note [44]. Furthermore, a 10[μH] choke and 120[Ω] at 100[MHz] ferrite bead were placed in series with the analog power input. This LC filter supported by the bead should effectively eliminate both low and high-frequency interference.

The clock and data lines of both I<sup>2</sup>C busses are equipped with standard 4.7[kΩ] resistors. Multiple 22[Ω] resistors were placed in series with high-speed clock signals of the SPI interface. Two 0[Ω] resistors are present on *FAULT* and *MODE* lines to facilitate an optional hardware isolation. A 10[kΩ] resistor at *PH3* is suggested by [44].

### ■ 4.1.2 PCB design

Location and fanout of the MCU are shown in figure 4.2. The MCU is placed on the PCB top side, covering most of the non-payload area. This big footprint of a LQFP144 package (approximately 2 x 2[cm]) is a consequence of avoiding the BGA packages while still trying to keep the pin count high. All of the capacitors were placed as close to their assigned pins as possible. In some cases, it was necessary to use the bottom side of the PCB. The same approach was applied to all of the resistors. A hole of 1.2[mm]

diameter is placed roughly at the middle of the MCU footprint. The diameter was set to fit a 19 gauge needle attached to a syringe with epoxy. This epoxy glue should be filled through this hole into the void space between the PCB and the MCU. This procedure is typical for space applications. Its purpose is to add some mechanical robustness to the LQFP device and create a thermal bridge between the PCB and the devices.

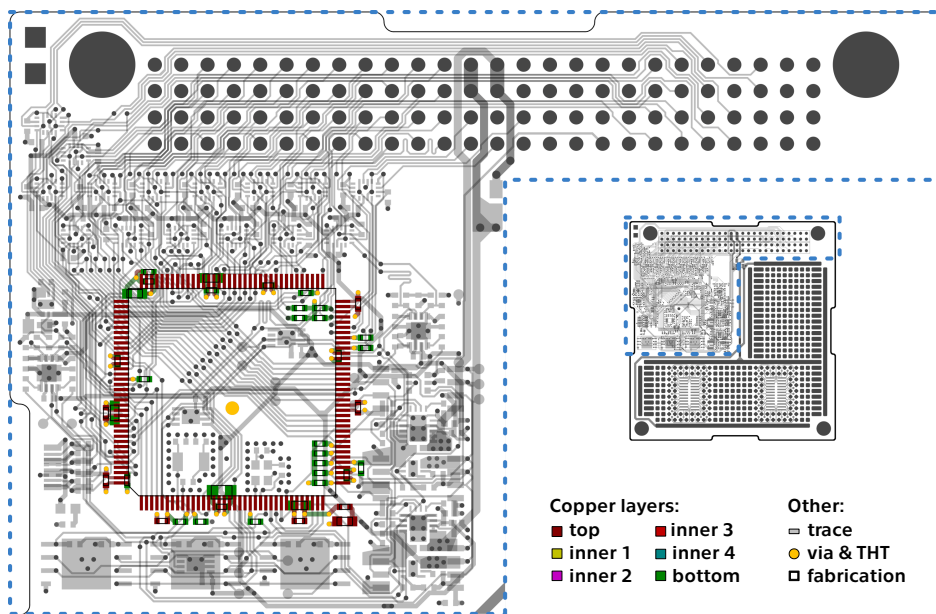


**Figure 4.2.** Highlighted location of microcontroller circuitry.

## 4.2 External clock sources

Proper timing and synchronization are the key features while dealing with high-speed data busses, ADCs, or other precise applications. The MCU is equipped with two internal RC oscillators that can be used to drive a master system clock and other auxiliary clocks [43]. These internal oscillators generally have a significantly lower frequency stability, a higher temperature dependency, and smaller overall accuracy than their external equivalents [45]. Therefore, to increase the clock precision and reliability in the harsh space environment, we had to implement external clock sources.

A 4 – 48[MHz] high speed external oscillator (HSE) can drive the system clock. Supported types are crystal, ceramic resonator, or silicone oscillator [43]. The last option seems to be the best as it is insensitive to electromagnetic interference (EMI) and vibration. The only downside is its slightly lower temperature rejection [46]. We chose the SiT8924B, a 26[MHz] silicon microelectromechanical system (MEMS) oscillator [47]. Accordingly to the clock configuration tool of the stm32cube software, we can reach various system clock and auxiliary clocks frequencies up to 78[MHz] (maximum is 80[MHz] [43]). This is done using the phase-locked loop (PLL) clock generation.

A 32.768[kHz] low speed external oscillator (LSE) can drive the real time clock (RTC), hardware auto calibration, or other timing functions [43]. Table 7 in [48] recommends individual crystal resonators for combination with STM32 MCUs. After a consideration of these options, we decided to pick the ABS07AIG ceramic base crystal [49].

### 4.2.1 Schematic design

The HSE circuitry follows the oscillator datasheet [47] and is shown on the right side of figure 4.3. Only a decoupling capacitor and a terminator resistor are required. The clock output *OSE\_IN* can be enabled or disabled by the binary *OSC\_EN* signal.

The LSE circuitry is based on a reference design in the oscillator design guide [48]. To achieve a stable frequency of this Pierce oscillator, it is required to find the values of load capacitors  $C_{L1}$ ,  $C_{L2}$  and external resistor  $R_E$ . This can be done using equations

$$C_L = \frac{C_{L1}C_{L2}}{C_{L1} + C_{L2}} + C_S \quad \wedge \quad C_{L1} = C_{L2}, \quad (1)$$

$$R_E = \frac{1}{2\pi f C_{L2}}, \quad (2)$$

where  $C_L$  is the crystal load capacitance,  $f$  is the crystal oscillation frequency and  $C_S$  is the stray capacitance [48]. Values of  $C_L$  and  $f$  are listed in the crystal datasheet [49]. We can assume as a rule of thumb, that  $C_S = 4[\text{pF}]$ . The final LSE circuitry with computed values of the components is shown on the left side of figure 4.3.

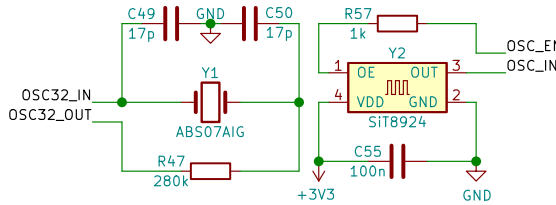


**Figure 4.3.** Schematic diagram of external clock sources.

### 4.2.2 PCB design

Location and fanout of the external clock circuitry are shown in figure 4.4. All of the components are placed on the bottom side of the PCB. The circuitry layout follows multiple tips presented in the oscillator design guide [48]. Separate GND planes are assigned to both the HSE and LSE circuitry. These planes are bounded by guard rings, formed by series of vias. Each of the planes is connected to a common GND only at one point. This approach provides proper EMI shielding while reducing a ground loop effect. We also minimized the distance between the MCU pins and both oscillators. All these measures combined should improve the clock generation stability and robustness.

## 4.3 Power management

The electric power subsystem (EPS) is known to be the most vital subsystem of a spacecraft [15–16]. Its reliability and error handling should be ensured by the power control and distribution unit (PDCU). However, it is a good practice by professional manufacturers to include an additional power monitoring and control to their OBC design [20–30]. We have to implement circuitry that can sense a power bus malfunction and, as a response, power down the OBC. This feature is also beneficial for some of the OBC on-earth user cases. During a hardware development or a presentation, the user might misconnect the power line or use an unsupported power source by a mistake.

A functional diagram of the implemented power management is shown in figure 4.5. To increase the overall efficiency and decrease complexity, we decided to avoid

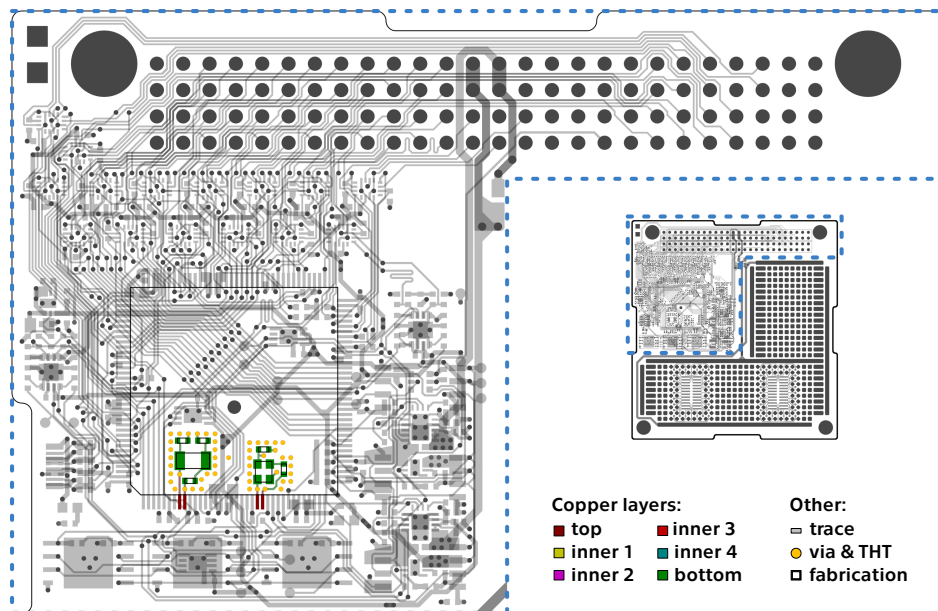


**Figure 4.4.** Highlighted location of external clock sources circuitry.

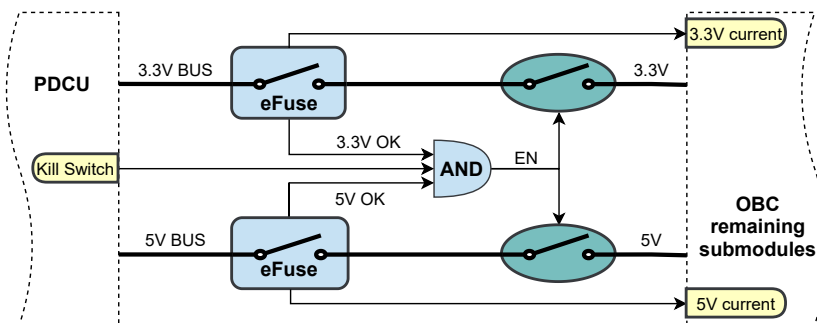


**Figure 4.5.** Functional diagram of power management circuitry.

any voltage conversion independent from the PDCU. Therefore, our OBC requires two separate inputs from the main power buss (3.3[V] and 5[V]). The OBC is connected to each of these inputs through an electronic fuse (eFuse). This device continuously monitors the bus for events of under-voltage, over-voltage, and over-current<sup>1</sup>. As a response to such an event, the eFuse will switch into high impedance and pull down specific input of an AND logic gate. This gate simultaneously controls two load switches, one for each power line. This approach ensures that a fault on one power bus will result in a high impedance of both OBC power inputs. It also eliminates the risk of a death loop, in which a reset of eFuses is not possible as they are switching each other off. Added benefits of this design are an inbuild current measurement and a Kill Switch integration into the logic gate. A summary of the final power management rating is listed in table 4.2. These values were chosen considering the power requirements of the remaining OBC components and are a subject of change by a future user.

### 4.3.1 Schematic design

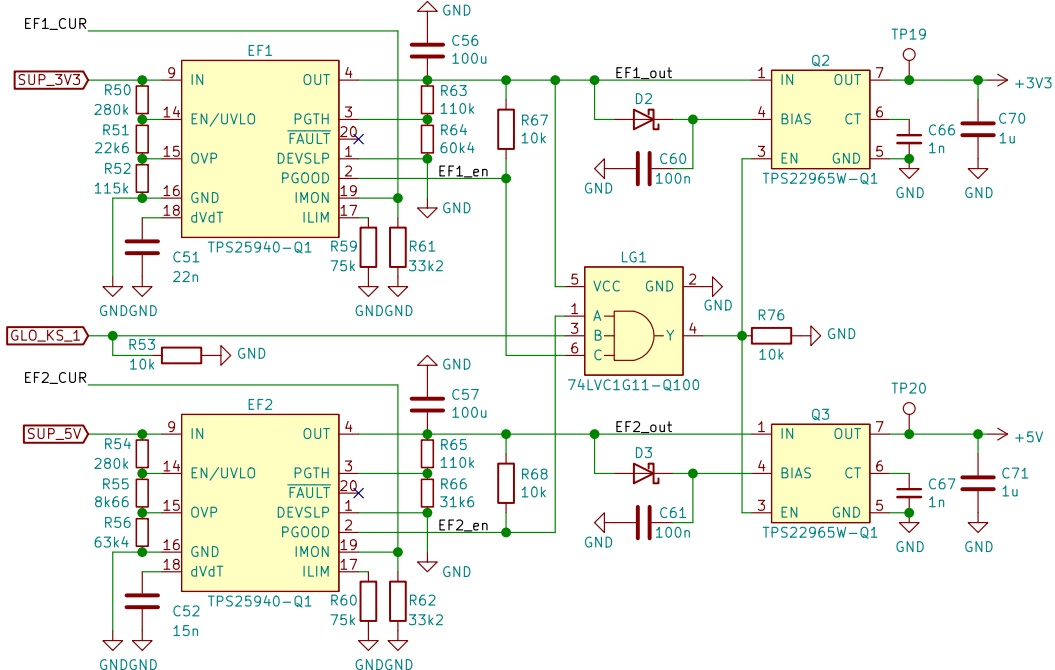
An actual schematic diagram of power management circuitry is shown in figure 4.6. The most important part of this design is the eFuse, as it covers all of the power control

<sup>1</sup> This is a crucial feature in handling and resolving a latch-up event.

Power input	Parameter	Min	Typ	Max	Unit
3.3[V] BUS	voltage	2.9	3.3	3.5	V
	current	0.0	-	1.2	A
5[V] BUS	voltage	4.6	5.0	5.4	V
	current	0.0	-	1.2	A

**Table 4.2.** OBC power rating. Value out of range will cause a protective shutdown.

features. We decided to use the TPS25940-Q1 device [50]. Custom threshold values can be set following the typical application schematic in the datasheet [50]. This is done by connecting specific resistors, with values calculated using the TPS2594x design calculation tool [51]. As the logic AND gate, we chose the 74LVC1G11-Q100 [52]. This device is designed to operate in a mixed logic level environment, what corresponds with our application. The last important component is the load switch. In our case, the TPS22965W-Q1 with an inbuilt output discharge function [53]. For a correct operation of the switch, the *VBIAS* pin should stay saturated for a while after disconnecting the *VIN* voltage. We achieved this behavior by charging a capacitor connected to the *VBIAS* from the *VIN* through a Schottky diode. Four reservoir capacitors are placed on both sides of the load switches, following the suggestions in both datasheets [50, 53]. Nominal logic values of all switching signals are set by pull-up or pull-down resistors.

**Figure 4.6.** Schematic diagram of power management circuitry.

### 4.3.2 PCB design

Location and fanout of the power management circuitry are shown in figure 4.7. All of the power management components are placed on the top side of the PCB. Similarly, all of the power tracks are on the top copper layer. Only a few signal traces are running within the second or the bottom layer. Both the 3.3[V] and 5[V] control circuitry share the same layout and routing regarding recommendations presented in the eFuse and

load switch datasheets [50, 53]. The 3.3[V] part is situated closer to the main PC104 header, while the 5[V] part is right below it. Both eFuses are connected to the main PC104 header power pins through strengthened 0.77[mm] traces in the third copper layer. Considering a standard copper thickness of 35[μm], each of the input traces is rated to deliver up to 2[A] of current. The logic gate with associated pull-down resistors is located above all of the remaining circuitry, closest to the main PC104 header.

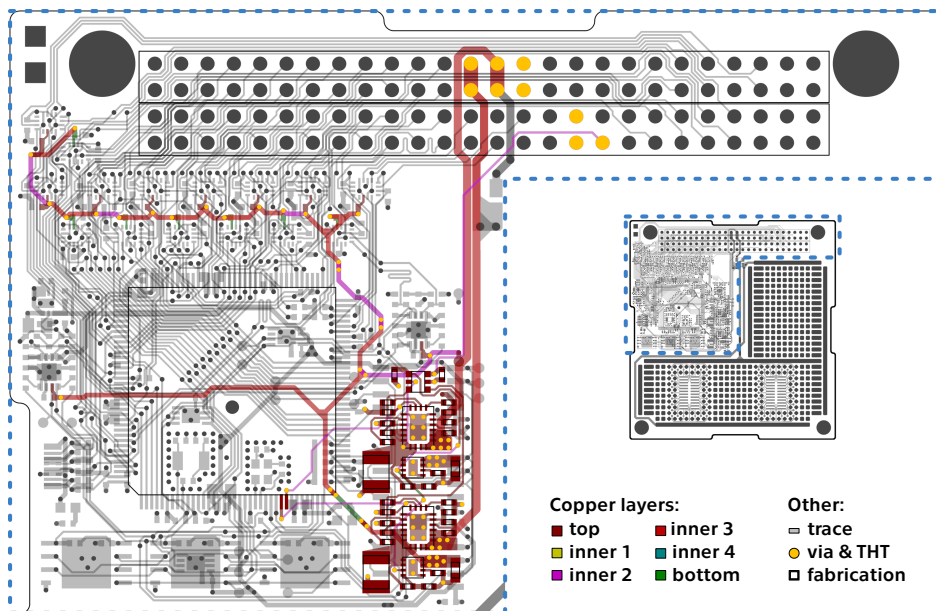


**Figure 4.7.** Highlighted location of power management circuitry.

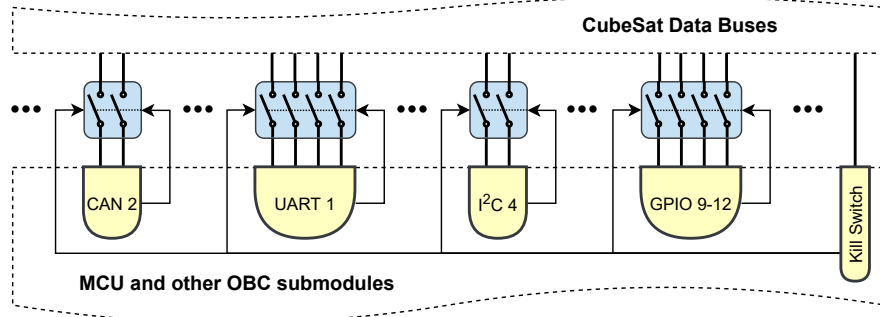
## 4.4 Peripheral isolators

The spacecraft OBC is connected to many data buses shared among all other CubeSat submodules. In some scenarios, the OBC must be able to isolate itself from a specific or multiple data buses. For example, to switch between OBCs in a redundant configuration, to handle a failure on a data bus, or to prevent unintentional interference. Standard approaches to address this feature are based on using analog switches [54], optocouplers [55], or FPGAs [20]. Furthermore, these isolators should also guarantee that all data lines are in a high impedance state when the OBC is powered off.

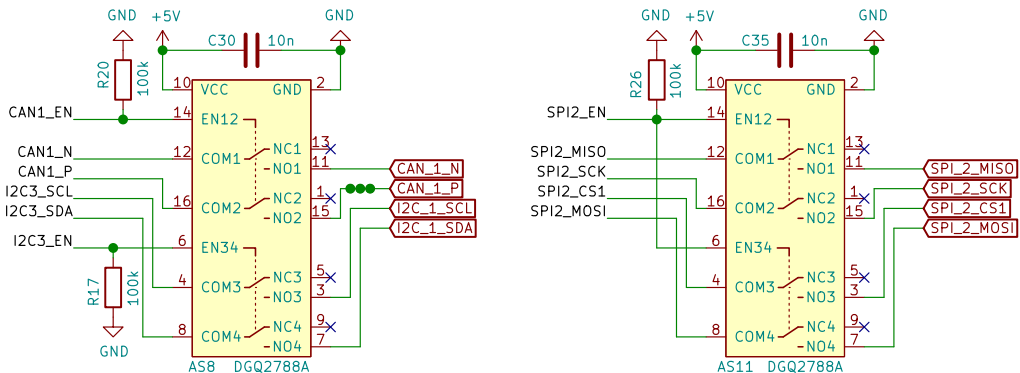
After a brief survey, we decided to implement the design using robust analog switches. This approach is more straightforward, less expensive, and requires a smaller PCB area than the optocoupler or the FPGA-based ones. A functional diagram of the implemented circuitry is shown in figure 4.8. All of the OBC data lines are connected to the rest of the spacecraft through a series of analog switches. These data lines are grouped by particular data buses and are assigned to a separate switch. The OBC can enable or disable a specific switch and therefore isolate a particular data bus from the remaining spacecraft subsystems. Pulling low the Kill Switch will result in high impedance of all switches and completely isolating the OBC data lines.

### 4.4.1 Schematic design

Schematic diagrams of two isolators are shown in figure 4.9. We decided to use the DGQ2788A device [56]. The OBC hosts fifteen of these analog switches in a dual double pole double throw (DPDT) configuration. The OBC data lines are connected to

**Figure 4.8.** Functional diagram of peripheral isolators circuitry.

common terminals (*COM*). Normally closed terminals (*NC*) are left floating, whereas normally open terminals (*NO*) terminals are connected to the spacecraft data lines. The important Kill Switch functionality is implemented using the device's power down protection. If the switch loses power, it will enter the normal state. This approach simplifies the circuitry a lot as it substitutes an otherwise necessary system of multiple logic gates. Other beneficial features of this analog switch are a high latch-up current of 300[mA] and inbuild signal clamping. The device will clamp all of the signals exceeding its supply voltage by internal diodes. As the MCU pins connected to these analog switches are 5[V] tolerant, we chose to power the switches from the 5[V] power bus. A malfunction could be caused by the switch's enable terminals (*EN*), as they do not include internal pull-up or pull-down resistors. We decided to use external pull-down ones to avoid the enable signals' floating state and avoid unintentional device switching. The decoupling capacitors were placed accordingly to the device datasheet.

**Figure 4.9.** Schematic diagram of two peripheral isolators.

## 4.4.2 PCB design

Location and fanout of the isolators circuitry are shown in figure 4.10. Sixty separate signals are running from the MCU pins through analog switches up to assigned pins in the PC104 header. Hence this part of the PCB was the most challenging to design. The switches are placed in two main rows, each on one side of the PCB (only two switches are not aligned). The position of every switch was determined by its assigned MCU and PC104 header pins. It took several iterations to find out the current layout. The routing network is quite dense, using all three copper signal layers. To accommodate all of the signal traces, the standard signal trace width was decreased from 200[μm] to 173[μm]. This new value was acquired as a maximal width possible to squeeze three

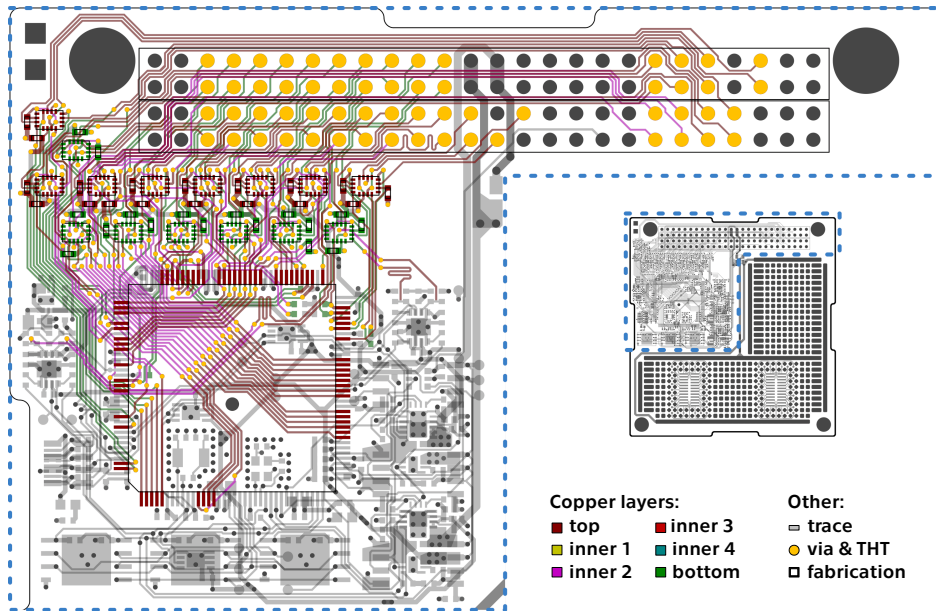


**Figure 4.10.** Highlighted location of peripheral isolators circuitry.

traces between two pins of the PC104 header. To ensure CAN buses signal integrity, we addressed a length matching of its differential pairs. As a finishing step of the routing, lengths of separate CAN traces were measured and tuned with serpentine patterns.

## 4.5 External memory

One of the OBC's important tasks is collecting and processing data from other sub-modules present in the spacecraft. As this payload and housekeeping communication might generate a wide data flow, external memory storage is usually dedicated to the MCU [20–30]. This secondary memory should be writable, preferably fast, and non-volatile (can retain the stored information after power off) to support quick buffering and permanent data storage. Commonly used semiconductor memory technologies matching the criteria are EPROM, EEPROM, FLASH, and various NVRAMs.

A great threat to memory storage is space radiation, as presented in section 3.1.1. In a single event upset (SEU), the storage node charge in memory is upset due to particle strike and change its logic level [35]. This effect results in random bit-flips throughout the memory address space, corrupting the stored information. Approaches handling this damage are based on i) more durable or even rad-hard memory ICs, ii) triple modular redundancy, and iii) error detecting and correcting codes. As the last approach is a software implementation, only the first two could be used in our design.

The EPROM and EEPROM memories are not a good candidate for the OBC, as they proved to be more sensitive to gamma radiation [37]. The same applies to MRAM, as these memories are generally sensitive to single event effects (SEE) [57]. On the other hand, the cell of fairly popular FLASH devices proved to be robust against SEU because more energy is required to change the state of a bit. FLASH memories are more tolerant to radiation and are a good candidate for vital data and code [14]. F-RAM is a technology that combines the best of Flash and SRAM. It offers faster writes, high read-write cycle endurance, and very low power consumption [58]. Moreover, the F-RAM memories have excellent tolerance to radiation [14]. Considering the listed aspects of radiation effects rejection, together with speed and power consumption, we

Subsystem	Size	Max. clock	SPI connection
FLASH	3x 32[MB]	133[MHz]	SIO, DIO, QIO, QPI
F-RAM	3x 2[Mb]	25[MHz]	SIO, QIO

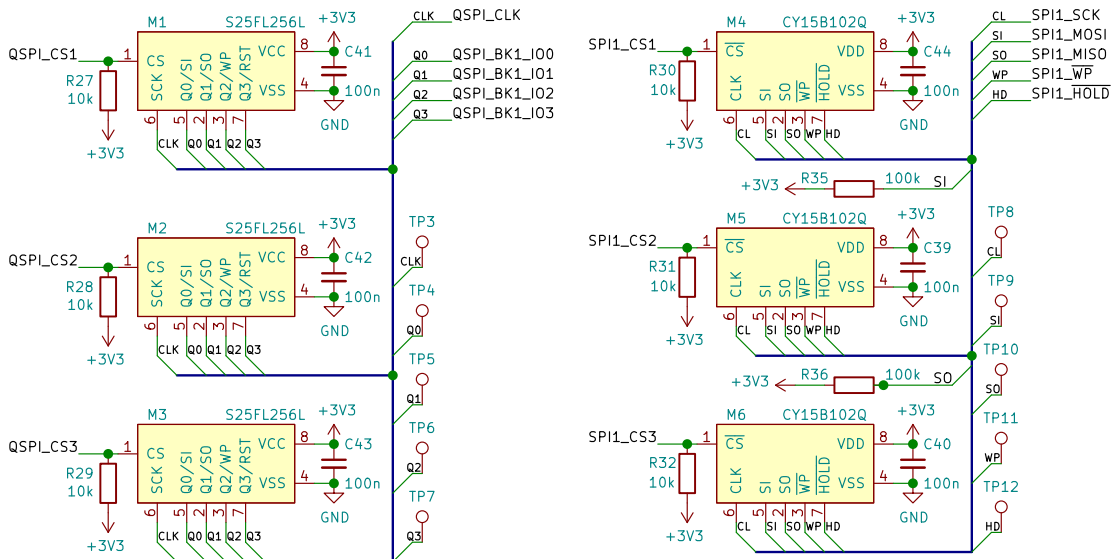
**Table 4.3.** Parameters of the external memory subsystems.

decided to include both FLASH and F-RAM memories in our OBC design. The final parameters of the external memory subsystems are listed in table 4.3.

### 4.5.1 Schematic design

Schematic diagrams of FLASH (left) and F-RAM (right) memory subsystems are shown in figure 4.11. Triple modular redundancy is achieved in both of them by connecting three of the same memory ICs to one shared data bus. The MCU can separately enable or disable a particular IC throughout its chip select (*CS*) pin. External pull-up resistors added to these selection lines set the disable mode as a default one.

As a FLASH memory, the S25FL256L device was selected [59]. The SPI interface of this 32[MB] NOR memory (also available in 16[MB] version) can operate in single, dual, or four-bit wide signal lines and also supports the quad peripheral interface (QPI) commands. For the F-RAM device, we chose the CY15B102Q [60]. This 2[Mb] memory supports a dual or four-bit wide SPI interface. The 100[nF] decoupling capacitors connected to the power inputs of the memory ICs were suggested by both devices datasheets. Additionally, a test point was placed on each signal line of both SPI data buses. This addition may improve the potential debugging of these subsystems.

**Figure 4.11.** Schematic diagram of external memory circuitry.

### 4.5.2 PCB design

Locations and fanout of external memory circuitry are shown in figure 4.12. Devices of the FLASH subsystem are located at the top side of the PCB, below the MCU. Devices of the F-RAM subsystem are located at the bottom side of the PCB, right from the MCU. This device is the only one in the entire OBC design with a non-fine pitch package. All of the SPI test pads are placed from the bottom side of the PCB.

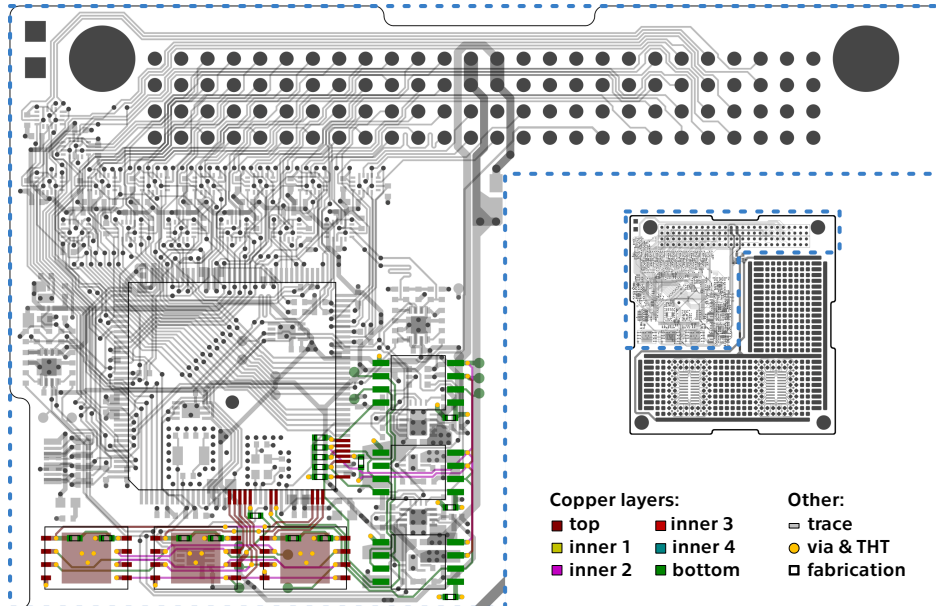


**Figure 4.12.** Highlighted location of external memory circuitry.

## 4.6 CAN bus drivers

The high-speed SpaceCAN is considered a primary control and monitoring bus of a LibreCube spacecraft. Therefore it was required to ensure its full support by the OBC. An external CAN transceiver is usually added to a microcontroller, as its internal physical layer has only limited properties or does not even exist. The separate transceiver provides a stable and reliable physical environment. In our case, the MCU's BxCAN is compatible with both 2.0A and 2.0B CAN specifications with a bit rate up to  $1[\text{MB s}^{-1}]$  [43]. As the MCU's CAN drivers are equipped with the 2nd network layer only, an external transceiver implementation to our design was required.

### 4.6.1 Schematic design

A schematic diagram of implemented CAN driving circuitry is shown in figure 4.13. As the MCU supports two independent CAN busses, we had to accommodate each of them. For the CAN transceiver, we decided to use a TCAN1051V-Q1 device [61]. The Rx/Tx lines of the MCU are connected to the device with a  $22[\Omega]$  terminating resistors. A test point is also present on each of these lines to assist potential debugging. This version of the device comes with a level shifting feature. Different voltage levels on CAN and Rx/Tx sides are supported. Since the SpaceCAN is a  $5[\text{V}]$  bus and the MCU operates at  $3.3[\text{V}]$ , we set the device's power levels accordingly. As recommended in the device datasheet, decoupling capacitors were added to power pins. Considering the CAN bus's importance, we expect it to stay active straight from powering on the OBC. To save some complexity and MCU pins, we decided to ignore the option of controlling the device standby mode. A pull-down resistor on the *STBY* pin forces an active mode.

A well-designed CAN network usually contains a terminating resistor, filtering, and a transient & ESD protection. To correctly implement these optional features, we followed application reports [62–63]. Instead of a simple  $120[\Omega]$  terminating resistor, we chose a more advanced terminating node. A difference is in added filtering as the node consists of two  $60[\Omega]$  series resistors connected to a GND through a  $4.7[\text{nF}]$  capacitor. Furthermore,  $100[\text{pF}]$  filtering capacitors were added to signal lines. Recognizing the

suggestions in the reports, we did not include any common-mode chokes or ESD protection in our design. Since our OBC is not intended to operate near heavy machinery, no extra improvement of susceptibility to electromagnetic disturbance or EMC is required.

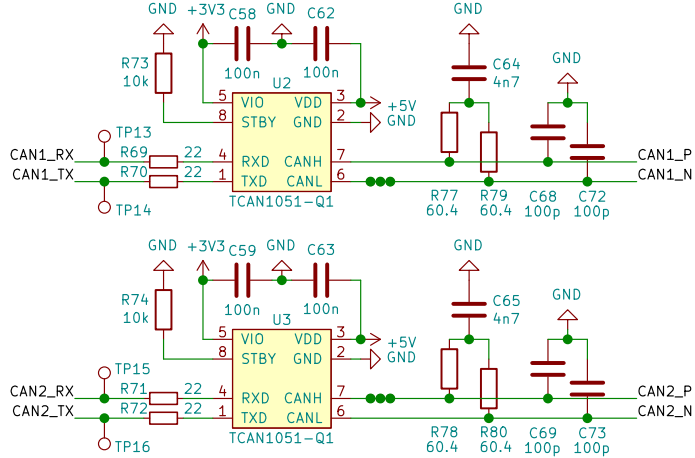


**Figure 4.13.** Schematic diagram of CAN bus driving circuitry.

## 4.6.2 PCB design

Location and fanout of the CAN bus driving circuitry are shown in figure 4.14. The transceivers are placed on the PCB top side in two different locations. Prioritizing the PCB surface's optimal usage, we were unable to keep the devices in a mutual area. The transceiver circuitry layout follows suggestions in the datasheet [61] and the application report [62]. This layout is the same for both devices. As mentioned in section 4.4.2, serpentine patterns were used to match trace lengths of particular differential pairs.

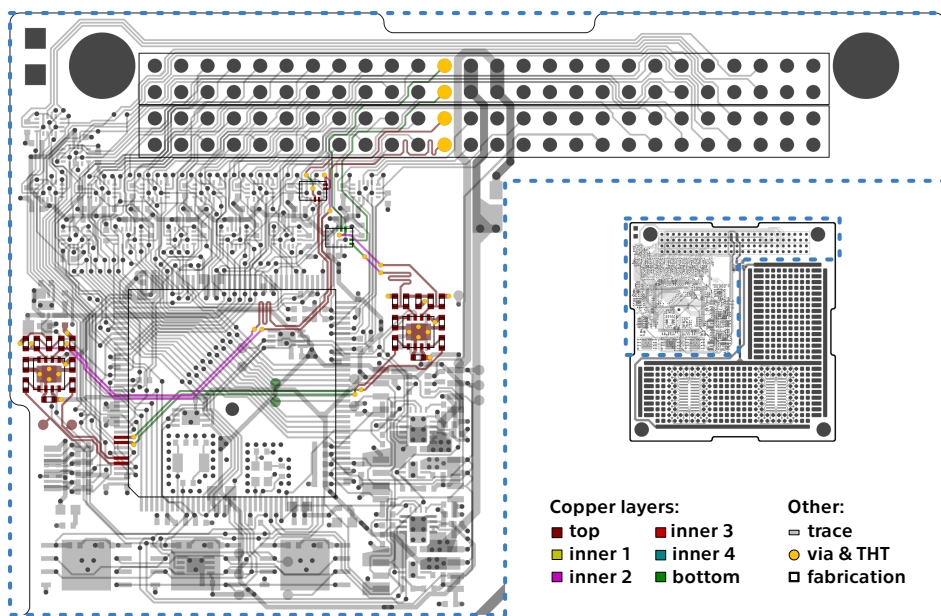


**Figure 4.14.** Highlighted location of CAN bus drivers circuitry.

## 4.7 Temperature monitoring

Temperature is a critical parameter in the space environment, and all electronic components are sensitive to its variation. Any increase in temperature may reduce their lifespan and even result in irreversible damage. Such a temperature increase can be evoked by an ambient temperature or by the component's activity. Most electronic components are designed to dissipate heat into the ambient air. This is problematic in the space due to its lack of an atmosphere. Instead, a component transfers heat into the PCB's thermal capacity.<sup>2</sup> This conduction can produce temperature gradients throughout the PCB and influence other components. Furthermore, a change in a component's temperature can indicate its malfunction. Sudden temperature increase is a common sign of a latch-up event [36]. Accordingly, the OBC temperature is a valuable part of a spacecraft telemetry and worthy of monitoring. Professional manufacturers have also included temperature sensors into their OBC [20–22, 25, 29–30].

Standard temperature sensor technologies include integrated circuit (IC) sensors, thermistors, resistance temperature detectors (RTDs), and thermocouples. Their key features are compared in the guide to temperature sensing [64]. The IC sensors appeared to be the best choice for our design challenge. These sensors are typical for their good accuracy, small footprint, easy complexity, and excellent linearity. A processing unit can usually communicate with the IC sensors using one shared data bus and receive ready-to-use temperature data. In contrast, the implementation of the other sensor technologies requires extra analog components and circuitry. For example, amplifiers and ADCs for thermistors and thermocouples or precise current sources and ADCs for RTDs. These non-IC technologies would also use multiple MCU pins and require additional calibration and shielding. As our goal was to design a compact PCB and a simple system, we decided to implement the IC sensors approach.

### 4.7.1 Schematic design

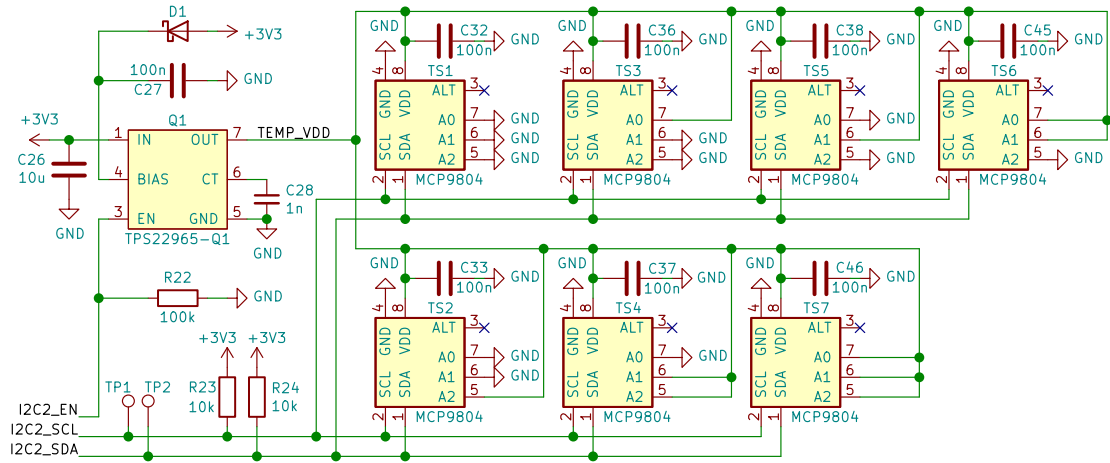
A schematic diagram of a temperature sensor network is shown in figure 4.15. After a brief survey, we selected a MCP9804 device [65]. This temperature sensor has an accuracy of  $\pm 0.25^{\circ}\text{C}$  and communicates through an I<sup>2</sup>C interface. The device offers eight different I<sup>2</sup>C addresses, selected by different logic levels on three slave address pins ( $A_0$ - $A_2$ ). Thanks to this feature, we were able to use only one I<sup>2</sup>C bus for all of the devices. The final address assignment to particular sensors is listed in table 4.4. As the temperature monitoring is continuous, we decided not to use the device's inbuild alter function. Placement of a decoupling capacitor and 10[k $\Omega$ ] pull-up resistors on I<sup>2</sup>C lines were suggested by the device datasheet. It is worth mentioning that this sensor supports a low-power standby mode, accessible through a special register.

Accordingly to the survey on CubeSat electrical bus reliability [34], the I<sup>2</sup>C interface is the most likely to fail. Over half of investigated spacecrafts experienced at least one I<sup>2</sup>C lockup<sup>3</sup>. Hence it was essential to apply measures assuring the proper functionality of our I<sup>2</sup>C based temperature monitoring network. We had to implement a mechanism that can either prevent the lockup from occurring or is capable of resolving it. We chose the second option, as we consider it as a more robust and reliable. A simple but efficient approach to resolve an I<sup>2</sup>C lockup is to reset the power of all its slave devices. For this purpose, we implemented the TPS22965W-Q1 load switch in the very same configuration as we have used in the power management circuitry (subsection 4.3.1).

<sup>2</sup> And then dissipated into the spacecraft environment by the thermal radiation [6].

<sup>3</sup> A continuous busy state of the I<sup>2</sup>C bus, where is the master prevented from starting a new transaction.

Designator	Targeted component		Slave addr.	I <sup>2</sup> C addr.
TS1	M2	- Flash memory	000	0x18
TS2	U1	- MCU, central west	100	0x1C
TS3	EF2	- 5[V] eFuse	001	0x19
TS4	U1	- MCU, north east	110	0x1E
TS5	U3	- CAN2 driver	010	0x1A
TS6	EF1	- 3.3[V] eFuse	011	0x1B
TS7	U2	- CAN1 driver	111	0x1F

**Table 4.4.** List of temperature sensors location and addresses.**Figure 4.15.** Schematic diagram of temperature monitoring circuitry.

### 4.7.2 PCB design

The layout of the temperature monitoring circuitry is dependent on the other subsystems. Therefore, it had to be implemented as the very last one. Each of the IC sensors was assigned to monitor a temperature of a particular device from another subsystem. These monitored devices were carefully chosen to cover all of the OBC's most critical components. These are various ICs used in the other subsystems as they execute multiple tasks, produce most of the heat, and are vulnerable to latch-up events. A listing of the monitored devices and their assigned temperature sensors is stated in table 4.4.

As we cannot exceed a total number of eight IC temperature sensors (MCP9804 devices) at one I<sup>2</sup>C bus, we decided to monitor only one of the three FLASH devices. We selected the one in the middle as a good approximation of the two remaining FLASH devices. None of the three F-ram devices is monitored directly as the opposite side of the PCB in their location contains a dense layout of the power management circuitry. However, the F-ram devices are neighbored by three temperature sensors: TS5, TS6, and TS3. Measurements obtained from these sensors should be sufficient to monitor the F-ram devices. The MCU contains an inbuilt temperature sensor suitable only for applications that detect temperature changes only [43]. We decided to monitor the MCU with a pair of IC sensors as we prefer to measure the absolute temperature.

To ensure correct temperature measurement, we have to create a sufficient thermal bridge between the temperature sensor and its targeted device. A common approach is to place the sensor on the other side of the PCB, right opposite the device. A thermal bridge is then created using a set of PCB vias. This method is recommended

and described in the temperature sensors guideline for SMDs [66]. Its illustration for our use case is shown in figure 4.16. It is worth mentioning that the added vias help dissipate the heat into the PCB and are usually required by the device's datasheet.



**Figure 4.16.** Illustration of a thermal bridge between the temperature sensor and WSON package (left) or LQFP package (right). Legend: ① 6-layer PCB, ② targeted device, ③ IC temperature sensor, ④ measurement die, ⑤ via, ⑥ thermal pad, ⑦ epoxy resin.

Location and fanout of the temperature monitoring circuitry are shown in figure 4.17. All IC sensors are placed at the bottom side of the PCB, directly under their targeted devices. The load switch is located at the PCB's west-central part. The switch itself and most of its auxiliary components are placed on the top side of the PCB. The I<sup>2</sup>C bus signal traces and separate power bus runs between all of the sensors.

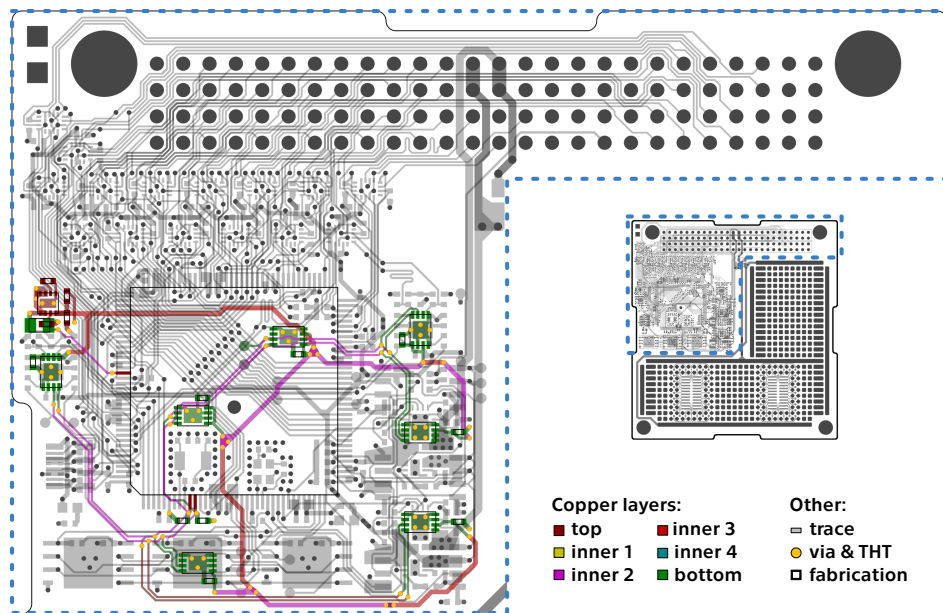


**Figure 4.17.** Highlighted location of temperature monitoring circuitry.

## 4.8 Debug connector

A host/target interface is required to program or debug the MCU. This interface is made of three components. A hardware debug tool, an SWJ connector and a cable connecting the host to the debug tool [44]. As the SWJ connector is a part of the target board, we had to implement it into our PCB design. The MCU has an embedded SWJ-DP interface that enables either a serial wire debug (SWD) or a JTAG probe to be connected to the target [43]. Considering that the SWD is required by the ST-LINK, is performed using two pins (five needed for the JTAG), and is the preferred debug port

[67], we decided to implement the SWD only. This decision slightly decreased the PCB complexity and freed some MCU pins for further usage. Also, the Sierra Board was not created with a mass production intent, the primary use case of the JTAG debug.

The implemented SWD connector includes not only the two mandatory SWDIO and SWCLK pins. An NRST signal is also presented, enabling a connection under reset. This signal is required to take back the control of the board when it is not responding [67]. Also, a serial wire output (SWO) is available, providing an asynchronous serial communication channel. It has to be used in combination with a serial wire viewer (SWV) [67]. Additionally, one UART channel is also presented, providing a convenient communication option for the development and testing process. Pin assignment of the ST-LINK compatible connector of the Board Sierra is shown in figure 4.18.

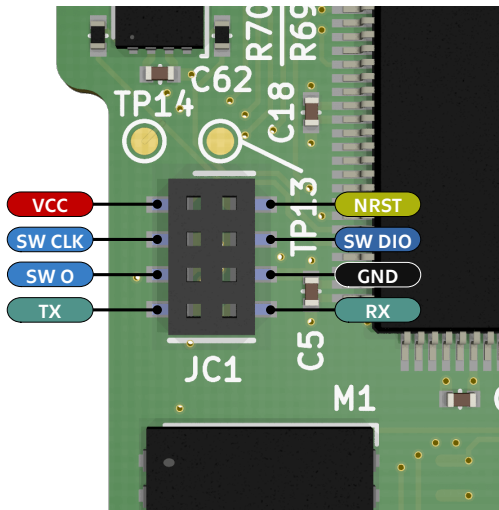


**Figure 4.18.** Debug connector pinout.

### 4.8.1 Schematic design

The programming connector is intended to be in direct touch with external hardware and human manipulation. As suggested in the application report [36], we decided to protect the associated signals against the ESD. A TVS diode array SP3012-06 [68] was selected, as it provides the exact pin count as needed. All of the debugging MCU signals were routed through this low-capacitance ESD protection device. A schematic diagram of the circuitry is shown in picture 4.19. Additionally, a  $22[\Omega]$  terminating resistor is connected in series to each signal. A  $100[\Omega]$  resistor and a ferrite bead are connected to the connector's power pin. Their purpose is to limit the transient current and suppresses high-frequency electronic noise that may affect the OBC from an attached debugger.

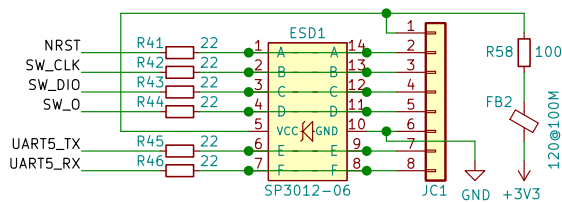


**Figure 4.19.** Schematic diagram of debug connector circuitry.

## 4.8.2 PCB design

Location and fanout of the debug connector circuitry are shown in figure 4.20. A small 4x2 female header with a 1.27[mm] pitch was selected as a debug connector. Its placement near the edge of the PCB in a cutout area should improve its accessibility and cable management. This SMD connector is located on the PCB's top side, while the remaining electronics parts are placed below it, from the bottom side of the PCB.

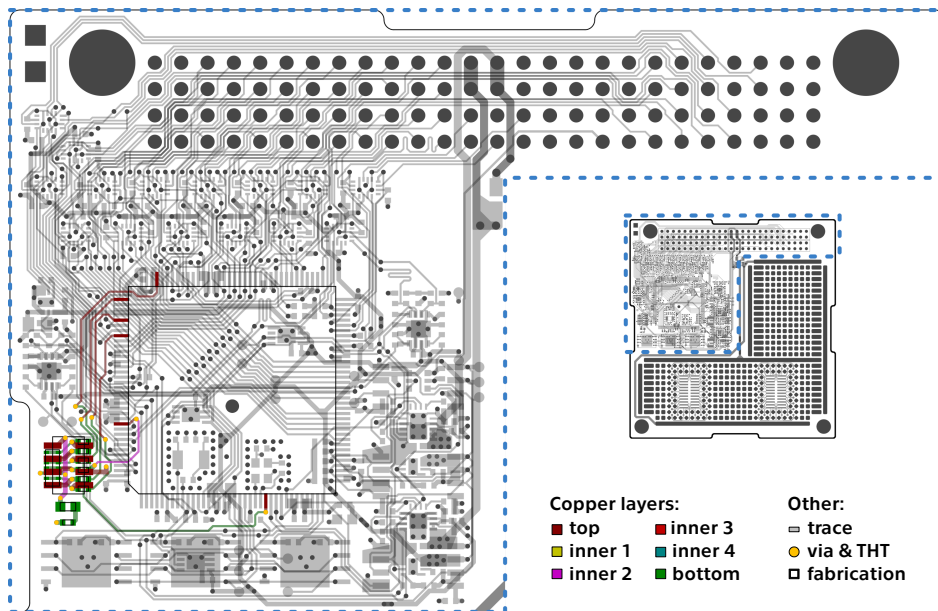


**Figure 4.20.** Highlighted location of debug connector circuitry.

## 4.9 Payload sector

As mentioned in section 3.3.2, only one-fourth of the entire PCB surface is occupied by the OBC circuitry. The remaining space is meant to be used as a user-defined payload sector. After discussing with the VST supervisors, we utilized this sector as a universal prototyping board. We implemented this feature to illustrate the purpose of this sector - to accommodate any user-specific circuitry. We expect that a future user of the Board Sierra would replace the universal board with his mission-specific circuitry.

The design of the universal prototyping board is visible in figures 8.9 and 8.10. Its main feature is a grid of 0.85[mm] wide THT holes with a plating utilized for an SMD soldering. This THT array is surrounded and divided by power bus rails, providing 5[V], 3.3[V], and GND connections. This power delivery is sourced directly from the main PC104 header, bypassing the power management circuitry. However, each of the rails is fused by a 1206 packaged ceramic fuse. In the lower part of the prototyping board, two universal SO-24 footprints are available on each PCB side for rapid prototyping. Every pad of these footprints is routed to a small circular pad for easier soldering.

# Chapter 5

## Board Delta

In this chapter, we address the Board Delta - a double redundant OBC module in the PC/104 format. We explain the motivation and expectation behind the redundant systems while providing description and comments on the schematic and PCB module design. A 3D visualization of the Board Delta is shown in figure 5.1.

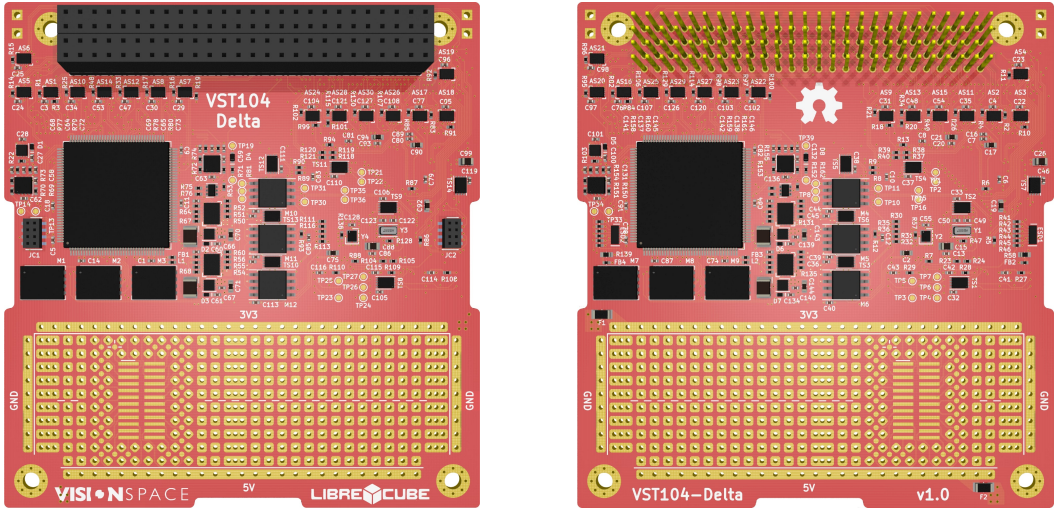


**Figure 5.1.** 3D render of the Board Delta from the top (left) and the bottom (right) side.

### 5.1 Motivation and expectation

During their launch and operation, Cubesats have to perform under extreme conditions of the surrounding environment. The most critical impacts were briefly described in the previous chapters, namely: i) damage of semiconductor devices caused by radiation (section 3.1.1), ii) exposure to wide temperature gradients and problems related to limited heat dissipation, and iii) significant mechanical stress generated by a launcher vehicle (both in section 3.2.1). Together with the practically non-existing possibility of maintenance, these problems are the key factors of a high failure rate of the already executed missions. As we have listed in section 2.1.5, every second launched Cubesat has experienced a fatal failure by 2016, from which 20% were caused by the OBCs.

Designing the particular modules with multiple layers of redundancy is a common method of increasing the spacecraft's overall reliability [16]. "By implementing onboard redundancy, CubeSats can meet or exceed their mission life, providing additional science data and post-mission payload testing." [9] Together with telecommunications, attitude determination, and electrical power, the OBC is one of the critical modules with high requirements for redundancy [55]. Some of the professional OBC manufacturers have also included elements of redundancy into their designs [20–22, 25, 28]. Interestingly, the fairly popular CubeSat OBC Kit from Pumpkin [24] is not one of them and its non-redundant architecture was pointed out as one of the two major weaknesses [34].

Although the Board Sierra implements some features of redundancy (triple external memories and dual peripheral data buses), it is still a single OBC module. In a case of permanent damage to the power management or the MCU, the Cubesat's mission would be severely jeopardized. However, this scenario can be eliminated by including another OBC into the module design. Each of these two OBCs is fully independent and has its own circuitry. Such a double redundant OBC module can simply switch between the two OBCs if one of them undergoes a serious malfunction. This approach was, for example, implemented in the professional DP-OBC-0402 by Data Patterns [20].

## 5.2 Double redundant design

From the beginning of the VST104 project, we thought about the Board Delta as a hardware merge of the two Board Sierras. The intention was to share the same OBC design between the two redundant OBCs at the Board Delta and also with the OBC on the Board Sierra. This approach of the only one OBC design has several advantages. Firstly, the two identical OBCs on the Board Delta can run almost the same software and provide the same functionality to the spacecraft. After an emergency switch to the other OBC, the Cubesat can continue to operate normally without changing the mission plan. Secondly, it allows an easy project migration between the boards. A potential user can develop and test his/her setup on the cheaper Board Sierra and then move to the more expensive Board Delta. Lastly, the approach also simplifies the development process and future maintenance of the VST104 project. It is faster and cheaper to develop and test out only one OBC design and then integrate it into different modules. Also, if an OBC design flaw or a possible improvement is found on one of the modules, it can be automatically implemented to the remaining modules.

### 5.2.1 Schematic design

As the idea was to use the already existing OBC design (described in chapters 3 and 4), the creation of the Board Delta schematic was straightforward. The KiCad project of the Board Delta consists of one primary sheet and two sub-sheets. The primary sheet contains the PC/104 header with assigned global signals, while each sub-sheet includes one OBC design copied from the Board Sierra. Power and peripheral input/outputs of these so-called Left and Right OBCs are attached to the same global signals as the PC/104 header. The resulting configuration of the module is simple: peripheral isolators and inputs of the power managements are connected directly to the PC/104 header. The individual peripheral isolators and Kill Switch function of the power management are then used to isolate and power down one of the OBCs.

Although we have stated multiple times that the OBCs share the same design, changes to a few PC/104 header pin assignments were required. The watchdog signal `CPU_WD_1` and the Kill Switch signal `GLO_KS_1` were assigned to the Left OBC, whereas their `CPU_WD_2` and `GLO_KS_2` variants were assigned to the Right OBC.

It is also important to note that our design does not exclude the possibility of running both of the OBCs simultaneously. In such a scenario, both OBCs should be powered on and negotiate the use of the shared PC/104 busses. The OBC not using a particular bus should isolate itself from it. The simultaneous operation can be beneficial in missions where significant amounts of data need to be processed quickly. Also, some Cubesats may require one primary OBC, handling the housekeeping and mission control, together with a secondary OBC, serving payloads such as scientific instruments or cameras.

## 5.2.2 PCB design

The decision to use only one OBC design does not apply exclusively to the schematic design but also to the PCB design. The same (or as similar as possible) PCB layout and routing of the OBCs would guarantee comparable mechanical, electrical, and thermal characteristics. As the desire to create the Board Delta was clear from the beginning, we count it into the design of the Board Sierra PCB. Its OBC was designed exclusively on the PC/104 module northwest quarter, leaving the northeast quarter empty.

We used several tricks to ensure the best possible similarity between the OBCs layouts. As a building template of the Board Delta PCB, we copied the final design of the Board Sierra. The OBC design on the template was assigned to the Left OBC. The layout for the Right OBC was generated using the Replicate layout plugin (mentioned in section 2.3.1). This plugin was capable of copying the entire OBC design, including all footprints, traces, and vias. However, to match the alignment and pinout of the PC/104 header, we had to flip this copied layout. This changed the previous top and bottom sides of the OBC and is why the MCUs are each on a different PCB side.

Some manual adjustments and routing were although required to finish the PCB design. The second and third inner copper layers were manually reversed back to meet the copper layers assignment from section 3.3.3. Also, the debug connector and its circuitry were mirrored back and rerouted. Thanks to this adjustment, both debug connectors are located on the PCB top side with the same orientation and pinout. However, the most challenging part was to manually trace all peripheral isolators to their required PC/104 pins. Multiple attempts and sacrifice of the northern edge cutout were required to accomplish so. The complex layout and routing of both OBCs are shown in figure 5.2. The Left OBC is located on the left side (northwest quarter), while the Right OBC is located on the right side (northeast quarter) of the Board Delta.

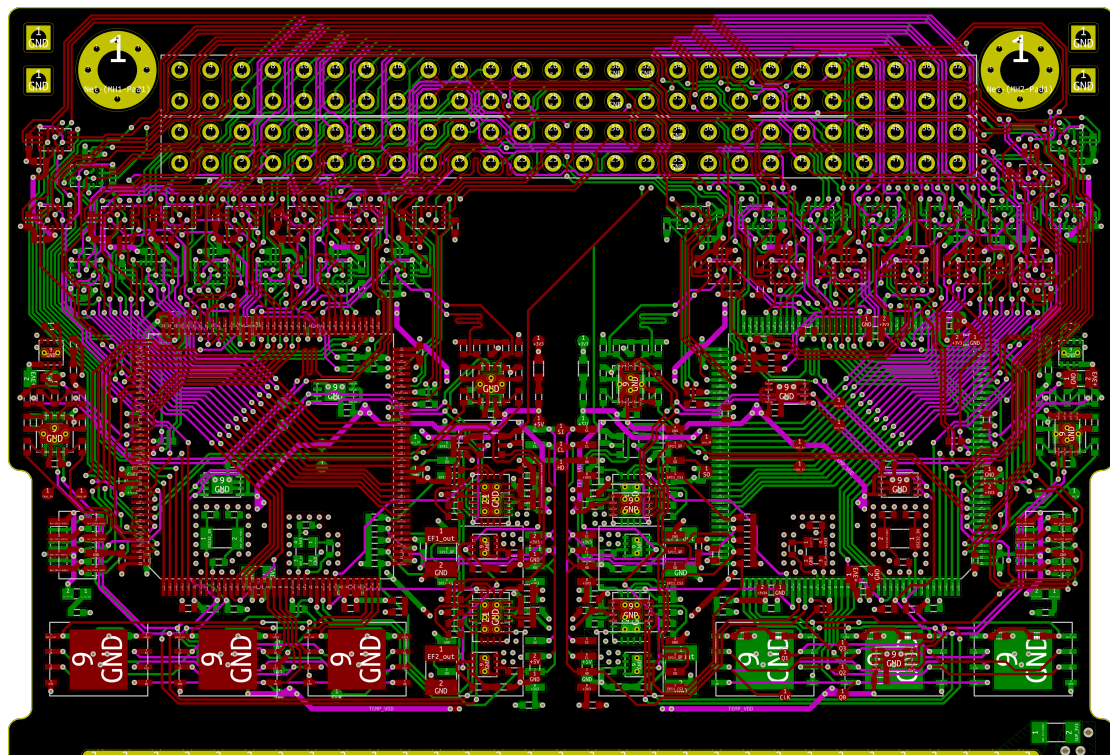


**Figure 5.2.** PCB design of the Board Delta captured directly in the KiCad environment. Visible is only the upper part with the PC/104 header and both OBCs.

# Chapter 6

## Element Foxtrot

This chapter addresses the design and characteristics of the Element Foxtrot - a FlatSat test bench for the PC/104 format modules with an inbuilt power supply. Its layout, embedded features, and functional principles are explained in the following sections. A 3D visualization of the Element Foxtrot is shown in figure 8.12.

### 6.1 FlatSat design

According to the VST desires, the Element Foxtrot fits two use-case scenarios. Like any other FlatSat, it supports the testing and development of new PC/104 modules. Also, it is a tool of their show-off and presentation. Developed modules can be attached to the FlatSat and then displayed at workshops or conferences. For example, running presented algorithms or software packages in real-time. Thus, we attempted to design the Element Foxtrot to accommodate handy features and have an appealing and professional look. After a discussion with the VST supervisors, we came up with its final design. The FlatSat has a rectangular shape and is divided into two parts.

The main part has dimensions of 20.25 x 26.10[cm] and hosts four slots for the PC/104 format modules. Silkscreen contours mark the position and orientation of these slots with respect to the LibreCube template (section 2.1.2). Individual slots headers are electrically connected together, concerning the VST104 pinout (section 2.3.4). A large VST company logo is displayed below the slots, giving the FlatSat a nice advertisement feature. The purpose of this part is to provide a connection between the mounted PC/104 modules while keeping them next to each other and easily accessible.

The second part of the FlatSat is an inbuilt power supply. The main task of this 20.25 x 4.55[cm] strip is to deliver power to the mounted PC/104 modules. This power supply can be connected to either a 6.4[mm] barrel jack or USB-C power inputs. Then, it delivers a 3.3[V], 5[V], and unregulated power lines. We decided to integrate a power source into the FlatSat to have an accessible power-up possibility. During a software testing or a conference, it might be convenient just to plug in an ordinary charger rather than setting up a laboratory power source or a battery-powered PDCU module.

The overall dimensions of the FlatSat are 20.25 x 30.75[cm], which should be easily fabricable by ordinary PCB manufacturers. If desired, the two FlatSat parts can be broken apart from each other and it is possible to use them separately. As the design of the inbuilt power source is nontrivial, it is addressed in the rest of this chapter.

### 6.2 Power supply features

Besides its main functionality, the power supply also offers multiple extra features. These small additions were designed to create the usage of the Element Foxtrot more convenient and user-friendly. The entities and locations of these features are shown and labeled in figure 6.1. We list and describe their functionality in the rest of this section.

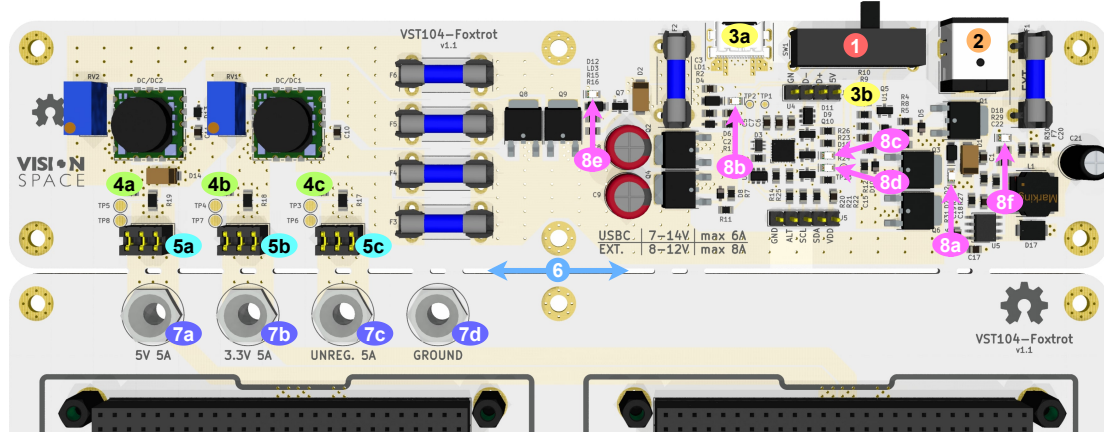


**Figure 6.1.** Visualization of the Element Foxtrot's power supply with its features labeled. Legend: ① input selection switch, ② 6.4[mm] barrel jack connector, ③ USB-C connector, ④ current sensing resistors: ④a 5[V], ④b 3.3[V], ④c unregulated, ⑤ disconnection terminal jumpers: ⑤a 5[V], ⑤b 3.3[V], ⑤c unregulated, ⑥ breakable connection, ⑦ 4[mm] banana sockets: ⑦a 5[V], ⑦b 3.3[V], ⑦c unregulated, ⑦d GND, and ⑧ indication & status LEDs (detailed explanation in section 6.2).

- **User control of inputs:** The inbuilt power supply supports two separate power inputs: a 6.4[mm] barrel jack or a USB-C connector. A three-position slide switch (on/off/on) between these two connectors is used to enable one or none of them. When its slider is located in the middle position, the power supply is turned off. When slid to one side, the corresponding power input enables, and the power supply turns on.
- **6.4[mm] barrel jack input:** This power input expects a positive barrel jack polarity. The supported input voltage range is 7-14[V], and the maximum current flow is 8[A]. The power input is embedded with a reversed polarity and overvoltage protection.
- **USB-C handshake input:** A standard USB-C connector is combined with a power delivery controller IC, allowing so-called handshaking. The power input can be used in two modes: i) it can handle an ordinary 5[V] USB-C charger, or ii) negotiate a power contract with an intelligent USB-C charger. Therefore, the supported input voltage range is 5 & 7-14[V], and the maximum current flow is 6[A]. The differential pair of the USB data bus is led to a separate header close to the connector. An independent 5[V] power bus is also available at this header. This feature allows the use of the USB-C connection also for communication purposes.
- **Current sensing resistors:** Before leaving the power supply and entering the other part of the FlatSat, the power lines are interrupted with shunt resistors. A 1206 sized SMD resistor's footprints are placed in series with those lines, accommodating an inbuilt current sensing feature. Two test pads are then connected to each resistor, providing a connection terminal for the voltage drop measurement. If not intent to use, the footprints can be populated with  $0[\Omega]$  resistors or even a blob of solder.
- **Disconnection terminal:** A set of removable jumpers can be used to temporarily separate the power supply circuitry from the rest of the FlatSat. Each of them is rated for currents of up to 6[A]. Although removing the jumpers would interrupt the power lines, the ground plane is shared and GND would remain connected.
- **Breakable connection:** Under some circumstances, it might be needed to remove the power supply from the remaining FlatSat entirely. In such a case, these two parts can be separated by breaking a connection between them. This line consists of multiple long cutoffs and can be broken with a reasonable amount of applied force.

- **4[mm] banana sockets:** A laboratory power supply with its standard banana cables can also be connected to the FlatSat. The 4[mm] female sockets are placed behind the power supply circuitry. These sockets will remain directly attached to the PC/104 modules power lines even after temporary or permanent separation of the power source. This can be used to bypass the power supply or for voltage measurement purposes. The sockets are available for all power lines together with the GND.
- **Indication & status LEDs:** To increase the user experience, a bunch of colorful light emitting diodes (LEDs) is spread through the power supply circuitry. Their monitoring purposes (following the labeling in figure 6.1) are: 8a - power at the barrel jack input detected (red), 8b - power at the USB-C input detected (red), 8c - a power delivery error (yellow), 8d - the power level negotiated successfully (blue), 8f - 5[V] bus for the USB-C data header active (green), and 8e - the power supply active (green).
- **Link to another Foxtrot:** In applications where more than four PC/104 modules are required, the PC/104 bus can be connected to another Element Foxtrot. This extension is made through two 45-conductor FFC cables. Their two SMD connectors are located under the third module of the FlatSat. It is important to note that these cables connect only the PC/104 data busses. The power delivery has to be connected separately, preferably using the 4[mm] banana sockets.

## 6.3 Power supply circuitry

A schematic diagram of the power supply circuitry is available at the end of the appendix section. This electronics scheme is rather complex, and it might not be easy to orientate in it quickly. Therefore we explain the circuitry design and functional principles with the help of its hardware diagram, presented in figure 6.2, instead.

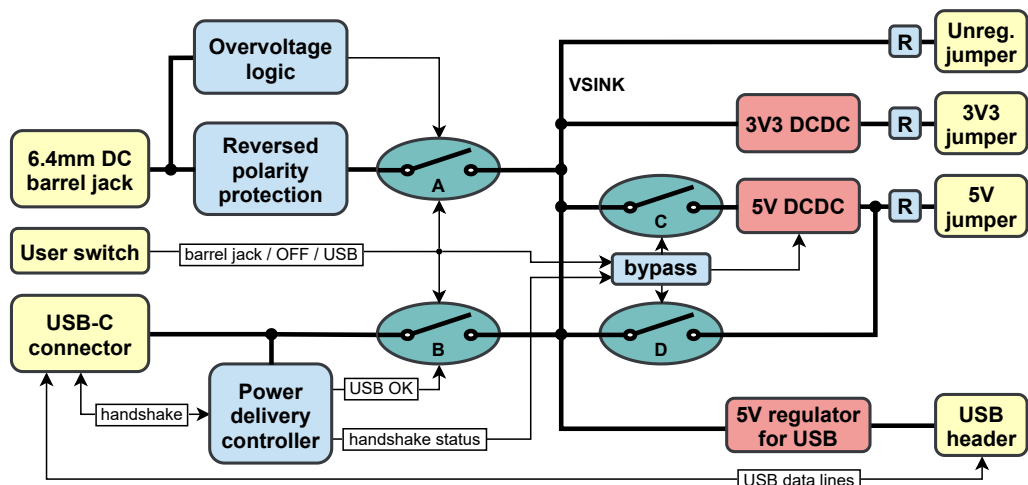


**Figure 6.2.** Diagram of the Element Foxtrot's power supply hardware architecture.

The central element of the circuitry is its main power bus, labeled as the *VSINK*. This bus provides electric energy for the rest of the FlatSat either directly or through the associated DCDC converters. This energy can be sourced in three different ways. In other words, the *VSINK* can be powered in three modes: i) from the 6.5[mm] barrel jack connector, ii) from the USB-C connector with power delivery, or iii) from the USB-C connector without power delivery. These modes are selected by a combined logic of the user switch position and the power delivery controller's handshake status.

In the first mode, a closed state of switch *A* and an open state of switch *B* are forced by the user switch position. In the real circuitry, these two switches (*A*, *B*) are implemented as bi-directional P-channel MOSFET switches. The first power mode also accommodates two safety features: overvoltage and reverse polarity protections. The overvoltage protection is designed to compare the input voltage and open switch *A* if it exceeds 15[V]. Its circuitry uses discrete components (such as TL432 voltage reference) and follows a reference design presented in [69]. The reverse polarity protection is based on a well-known design using a single P-channel MOSFET combined with a Zener diode.

The second and third modes share the same setup while powering the *VSINK* bus. The user switch forces an open state of switch *A* and permits a closed state of switch *B*. The associated power delivery controller makes the final decision whether to close or leave switch *B* open. In the circuitry design, we have implemented a standalone STUSB4500 controller accordingly to its typical application given in its datasheet [70] and the evaluation data-brief [71]. This device attempts to negotiate an appropriate voltage from the 7 – 14[V] range with the attached USB-C charger. If the charger supports power delivery and the negotiation is successful (mode ii) or if the negotiation is unsuccessful<sup>1</sup> although standard 5[V] is provided (mode iii), switch *B* is closed by a *USB OK* signal. The STUSB4500 device can be initialized through the I<sup>2</sup>C connection (using the associated header) as described in its programming guide [72]. We found the approach using the STSW-STUSB003 software library [73] to be the most convenient.

Once the *VSINK* bus correctly powered, it is required to distribute the power to the FlatSat's separate power lines. All of the PC/104 slots are connected to the required 3.3[V], 5[V], and unregulated lines. The unregulated line is attached to the *VSINK* bus directly. However, step-down DCDC converters are necessary to decrease the *VSINK* voltage for the 3.3[V] and 5[V] power lines. For this purpose, the OKL-T/6-W12 devices were selected. Output voltages of both converters are set by multi-rotation trimmers, enabling a fine tuning. Running the converters in the power modes i and ii is straightforward as the *VSINK* voltage is guaranteed to be at least 7[V]. This is above the 6.5[V] minimum required by the 5[V] converter. Yet, the mode iii is problematic as its *VSINK* voltage is only 5[V] and therefore insufficient. Hence, bypassing the 5[V] DCDC converter in the power mode iii had to be implemented. We accomplished this by including two more P-channel MOSFET switches (switches *C* and *D*) controlled by a *bypass* logic. Inputs of this logic are the user switch position and the *handshake status* signal from the power delivery controller. If the power from the barrel jack was selected (mode i) or the USB-C negotiation was successful (mode ii), the *bypass* logic closes switch *C* and opens switch *D*. However, if the power from the USB-C was selected and the negotiation failed (mode iii), the logic opens switch *C* and closes switch *D*. As mentioned in section 6.2, current sensing resistors (marked as *R*) and *jumper* terminals are placed between the power supply circuitry and the PC/104 slots.

Inspired by the data-brief of the STUSB4500 evaluation board [71], we decided to include a separate step-down switching regulator. The L7985 device is connected directly to the *VSINK* bus and provides a stable 5[V] output for the USB data connection.

Various ESD protection diodes, 2AG cartridge fuses, and reservoir capacitors are distributed through the circuitry. For their exact location, refer to the circuitry electronics schematic. A SPICE-based analog electronic circuit simulator LTspice was used to simulate and check for the desired functionality of the presented circuitry. This functionality was afterward properly tested on multiple assembled Element Foxtrots.

---

<sup>1</sup> The power delivery negotiation (*handshake*) can fail because of two reasons: the charger i) does not support power delivery, or ii) cannot provide voltage (current) from the required voltage (current) range.

## 6.4 PCB design

The Element Foxtrot is designed on a four-layer PCB with a slightly unconventional copper layer assignment. The two previously mentioned parts of the FlatSat (the power supply part and the main part with four PC/104 slots) are routed with different approaches, sharing only the common ground plane. The final layout and routing of the whole FlatSat captured from the KiCad environment is shown in figure 8.13. The location and layout of the power supply's circuitry are shown in figure 6.3. The location and layout of the power supply's circuitry are shown in figure 6.3.

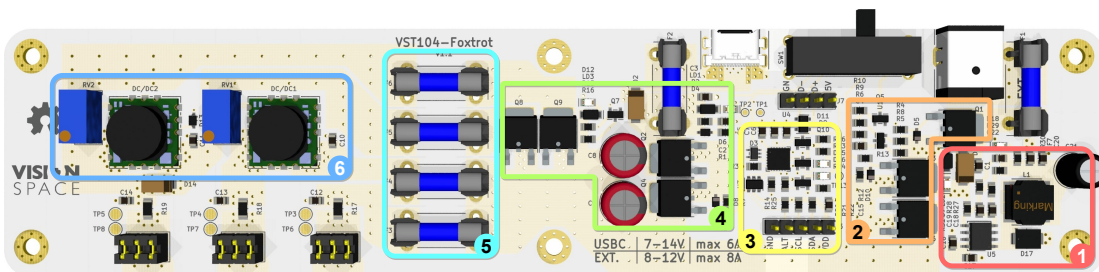


**Figure 6.3.** Location and layout of the Element Foxtrot's power supply circuitry. Legend: ① step-down switching regulator for the USB communication, ② barrel jack overvoltage and reverse polarity protection, ③ power delivery controller, ④ power source and bypass switching, ⑤ power lines 2AG cartridge fuses, ⑥ tunable DCDC converters.

In the power supply part, the top and the first inner copper layers are used for the power routing. Power busses and other power connections are formed from polygons of these layers. A dense rectangular net of vias is used to connect these layers within an individual bus. These power traces (polygons) are scaled to easily withstand a total current delivery of 6[A]. The second inner layer accommodates the common ground plane. All of the power supply electronic components are placed on the PCB top side for easier assembly. Therefore the top layer is also used for a majority of the signal traces. If it was not possible to route a trace there, then the bottom layer was used.

The main FlatSat part contains just a few power polygons but a very dense network of signal traces. These traces are placed on the top and the bottom copper layers. The first inner layer supports the power delivery, whereas the second inner layer is the common ground plane. The PC/104 slots are connected in a U shape, providing one continuous data bus avoiding any loops. The silkscreen numbers marking the individual slots are enumerated with respect to this connection. All of the signal traces connecting the slots had to be routed manually as all auto-routing attempts have failed.

# Chapter 7

## Board Sierra - testing

Functionality testing should be a part of every hardware development project. In this chapter, we briefly describe the testing tool we have developed for the Board Sierra together with the process and results of the already executed radiation testing.

### 7.1 Testing software

After assembling the first Board Sierra module, we had to ensure that it behaves as desired. A simple testing software had to be developed to loop through the separate subsystems while testing their proper functionality. To accomplish this, we decided to implement a small testing toolbox named **VST104-Testing**. This software package is written in a C language and developed in the integrated development environment STM32CubeIDE. Its current version includes the following tests:

- Enabling the HSE circuitry as a source for the MCU main clock.
- Reading the current consumption analog outputs of both eFuses.
- Switching on and off particular peripheral isolators.
- Enabling, configuring, and reading the inbuilt temperature sensors.
- Configuring, and reading manufacturer data from the FLASH ICs.
- Configuring, and reading manufacturer data from the F-RAM ICs.
- Writing to and reading from the FLASH memories using a QSPI.
- Setting up and maintain a simple CAN communication.

Outputs of these tests are in a form of logs sent throughout the SSW or the UART. The logs are divided into three groups: system information, error report, and data.

### 7.2 Radiation testing

As described in section 3.1.1, space radiation is a well-known hazard for CubeSats and electronic systems in general. Thus, we were particularly interested in how well the Board Sierra performs in a radiation-rich environment and what total dose it can overcome. Motivated by another project, we were also interested in similar characteristics of some COTS acceleration, angular velocity, and magnetic flux density sensors.

Thanks to the nuclear research institute ÚJV Řež a.s, we were given an opportunity to execute such an experiment. This section presents our testing approach and results obtained during exposure to a cobalt-60 gamma radiation source. After the experiment, the carried nominal ionizing radiation dose was determined as 49.0[Gy/hour].

#### 7.2.1 Experiment setup

For the purpose of the radiation testing, the Board Sierra was extended with four electronic sensors: i) an always-on 3D accelerometer and 3D gyroscope LSM6DS3, ii) 2x a high-performance 3-axis magnetic sensors MMC5983MA, and iii) an integrated 6-axis motion processor with gyroscope and accelerometer MPU6050. All of these sensors

were connected with the OBC throughout two I<sup>2</sup>C data buses. Each sensor was powered with a separate transistor controlled by the OBC. A proper power reset of each sensor could have been achieved by turning off this transistor and isolating the corresponding I<sup>2</sup>C peripheral isolator. This feature was implemented in order to resolve a potential bus lockup or the sensor's latch-up. A PNP transistor with a lower amplification factor and a saturated base current was selected to minimize the failure of this system.

During the entire experiment, two independent UART channels with separate FTDI TTL-232R converters were used for recording the OBC's logs. On top of that, we decided to measure the current consumption of the OBC's 3.3[V] and 5[V] power inputs together with the 3.3[V] input of the sensor board. For this purpose, three current monitoring resistors (shunt resistors) were attached as close to these power inputs as possible. The measurement of these currents in a 60[Hz] frequency was achieved with a data acquisition module PXIE-4303 DAQ installed in a PXIE-1082 frame.

A universal PC/104 module introduced in section 2.2.1 as a Board Zero was used to act as a test-bed for the sensors and their power switching circuitry. This sensor board was then mounted on a laminate sheet right next to the tested Board Sierra. An electric connection was established between the boards through ribbon cables. A labeled photograph of this setup is shown in figure 7.1. To accommodate the shunt resistors and distribute the power into the OBC, a small universal PCB was attached directly to the Board Sierra's PC/104 header. Each of the shunt resistors was assembled from seven high-precision SMD resistors connected in parallel, resulting in a total resistance of 1[Ohm]. This hardware setup was then inserted into the radiation chamber.

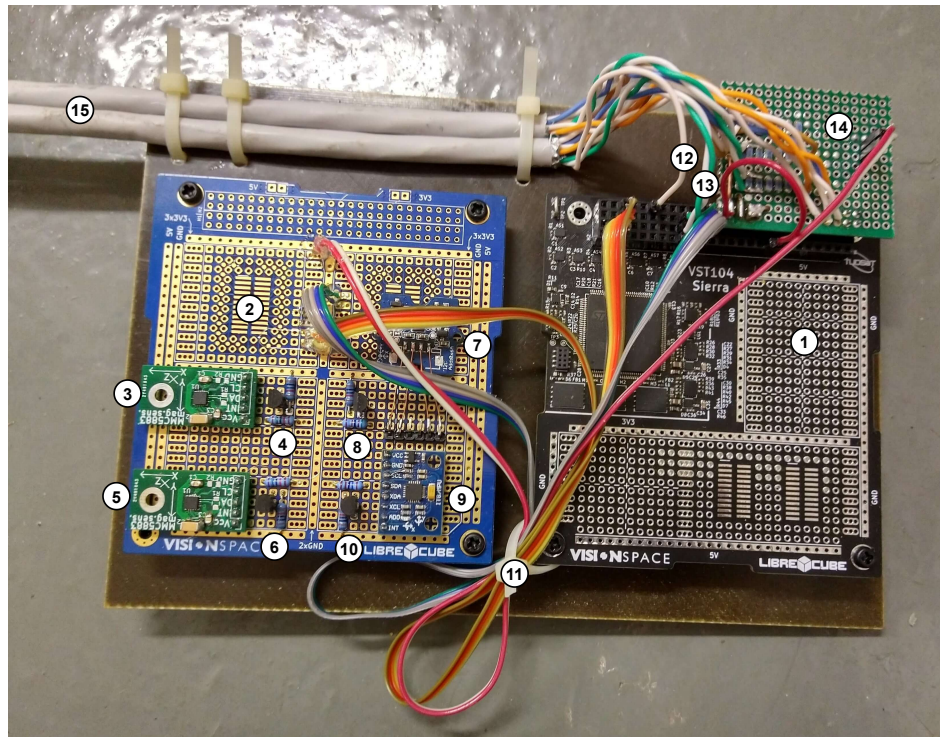


**Figure 7.1.** A hardware setup tested during the experiment. Legend: ① Board Sierra module. ② sensor board, ③ first MMC5983 sensor ④ with its power switching, ⑤ second MMC5983 sensor ⑥ with its power switching, ⑦, LSM6DS3 sensor ⑧ with its power stitching, ⑨ MPU6050 sensor ⑩ with its power switching, ⑪ ribbon cables providing connection between the boards, ⑫ watchdog signal wire, ⑬ UART TX wires, ⑭ universal PCB with the shunt resistors, ⑮ data and power cables reaching to a control room.

The testing software described in section 7.1 was used as a template for this experiment. In order to support all of the intended features, we had to extend its I<sup>2</sup>C drivers and modify its data-logging mechanism. All of the libraries needed to enable communication with the attached sensors were written by ourselves. By referring to the sensors' datasheets, we were able to create lightweight and robust minimal drivers. The benefit of this approach was the full control and customization of these essential functions. The logging templates were extended with new error identifiers, support of data triplets, and various system messages. The particular measurements and testing were conducted in one continuous loop, executed with a 2[Hz] frequency. Logs of system information, measured data, or potential errors were sent continuously. If a sensor reading encounters an error, the software forced the sensor hardware power to reset in the following loop. To decrease the risk of accumulating an electric charge, a prevention power reset of all sensors and isolators was conducted every ten minutes.

To enable a hard reboot from a possible system crash, a watchdog module was implemented as the last mean of the OBC recovery. In its active state, the OBC was permanently toggling a logic signal to indicate its well-being. The duration between the last two logic changes was continuously monitored and compared against a set threshold. If this threshold had been reached, a watchdog module disconnected both 5[V] and 3.3[V] power lines from a power supply for a couple of seconds. A photograph of the actual watchdog module is presented in figure 100. The design of this module was based on an STM32 Blue Pill board driving two electromagnetic relays.

## 7.2.2 Experiment results

Being a complex system of multiple semiconductor devices, the OBC was not expected to withstand the whole experiment. At 5.19[hour] after the start, the first unintentional reboot was logged. Until this point, the OBC performed normally without a single malfunction. The radiation dose at the time of this event was 254.32[Gy]. This reboot was the opening of 6.8 minutes long OBC's decay. Figure 7.2 shows timestamps of data and reboot logs received in this period. It is visible that the OBC entered a loop reaching up to 110 reboots per second. Despite this enormous frequency, some windows of inactivity and even a few data logs can be observed. At 5.27[hour], the OBC managed to start functioning again. Although, with visible delays between the acquired data. The very last log was received from the OBC at 5.30[hour], marking the end of its functionality. The overall radiation dose at this point was 259.90[Gy].

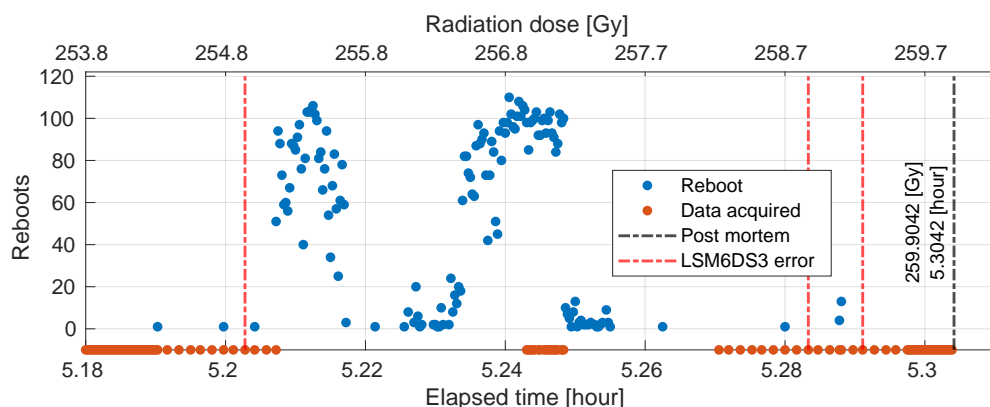


**Figure 7.2.** Timestamps of logs received from the OBC during its last moments of activity.

The OBC's and the sensors' current consumptions, measured through the external shunt resistors, are shown in figure 7.3. The periodically repeating pattern on both 3.3[V] power busses was generated by the prevention power reset. As this feature has powered off the sensors and suspended some of the OBC's activity every ten minutes, the corresponding decrease in required power is visible. Another noticeable trend is the increasing current consumption by the OBC and slightly decreasing current consumption by the sensor board. However, this time we cannot provide it with an explanation. A significant current drop and oscillations follow the already described OBC failure. Some changes in the current consumption are also visible closely before this event.

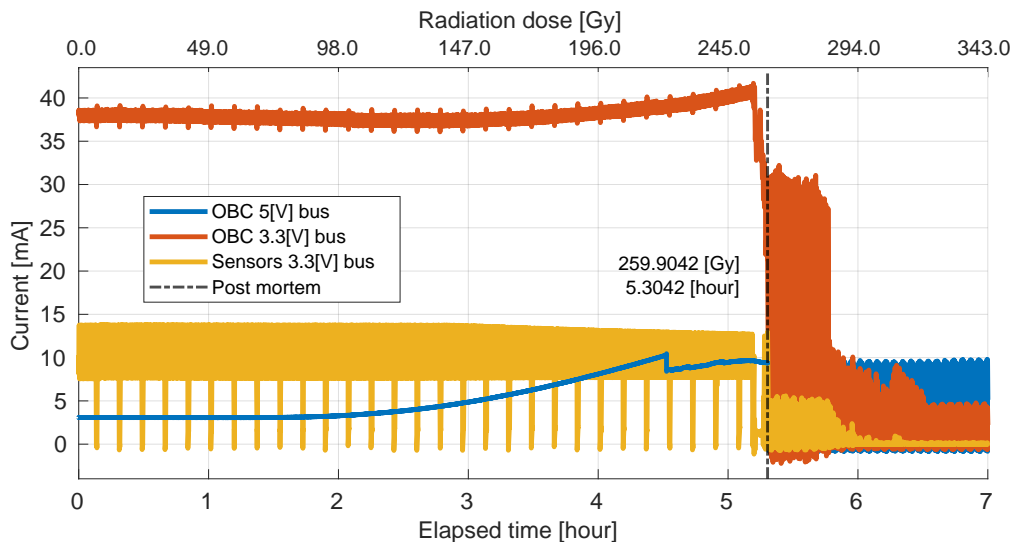


**Figure 7.3.** Current consumption measured throughout the experiment.

Temperature readings obtained from the OBC's inbuilt temperature sensors are shown in figure 7.4. No errors or failures of these sensors were recorded throughout the experiment. The acquired data also doesn't show any abnormality in the OBC's temperature or heat distribution. The slightly increased readings of the sensor T1 could be explained by its assignment to the Flash memory subsystem. Its continuous activity might have easily resulted in an increase of its temperature by roughly a  $0.75^{\circ}\text{C}$ .

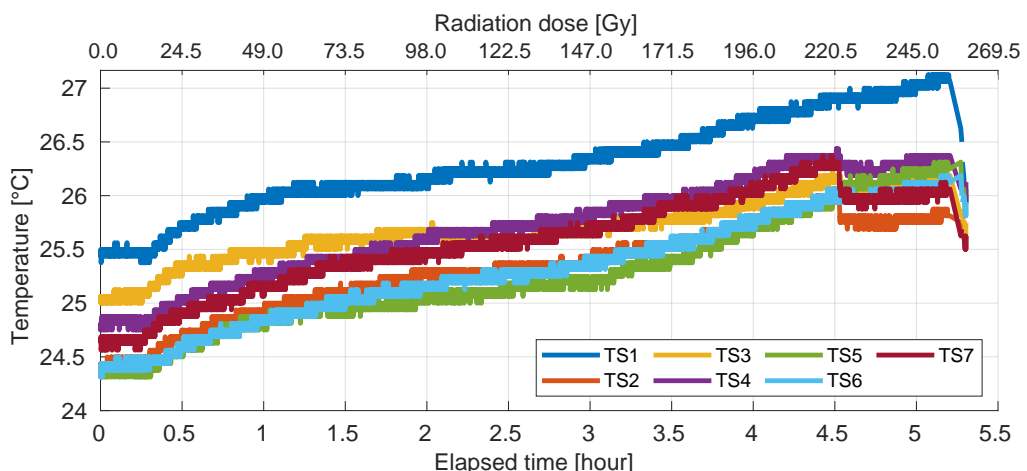


**Figure 7.4.** Readings of the OBC's inbuilt temperature sensors. The location and purpose of each sensor were described in section 4.7.

The LSM6DS3 was the only sensor that has experienced a total failure (actually seven of them). After being requested by the OBC, no response was obtained from the sensor, and the I<sup>2</sup>C connection timeout was reached. The first failure occurred after exposure to a radiation dose of 196.90[Gy]. Timestamps of these failures, together with the obtained angular velocity, are shown in figure 7.5. A continuous malfunction/degradation of the sensor is visible from these data, as the Y and Z-axis readings are decreasing over time. A real motion could not have caused these trends due to the sensor's stationary mount. Interestingly, the acceleration data acquired from this sensor are perfectly reasonable.

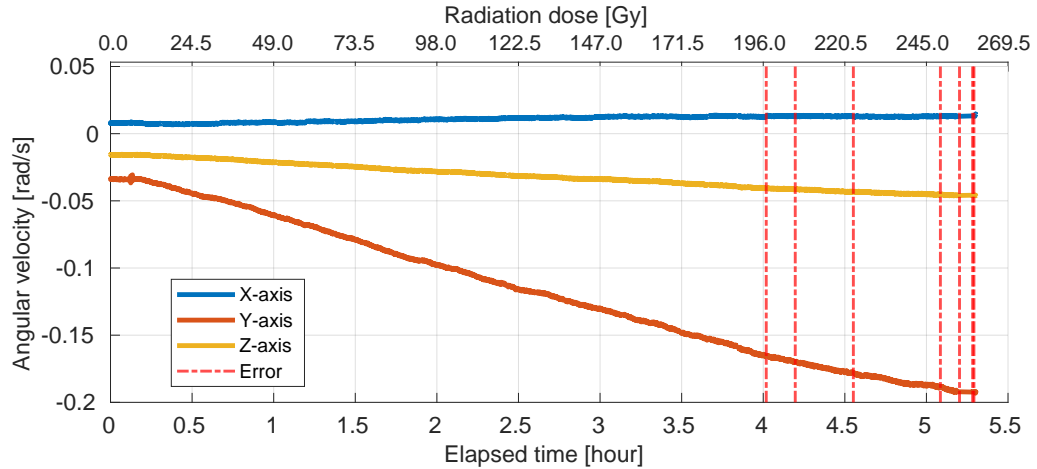


**Figure 7.5.** Angular velocity readings and occurred malfunctions of the LSM6DS3 sensor.

Similar progressive degradation of measured data has also occurred in the case of both MMC5983 sensors. Their magnetic flux density readings are shown in figure 7.6. Regarding the data, it seems that the slight drifts started to affect the Y and Z-axis simultaneously. This first sensor encountered this problem at 2.5[hour], followed by the second sensor at 3.0[hour]. Similarly to the previous LSM6DS3 sensor, any variations in the data could not have been caused by a change in the sensors' position or orientation.

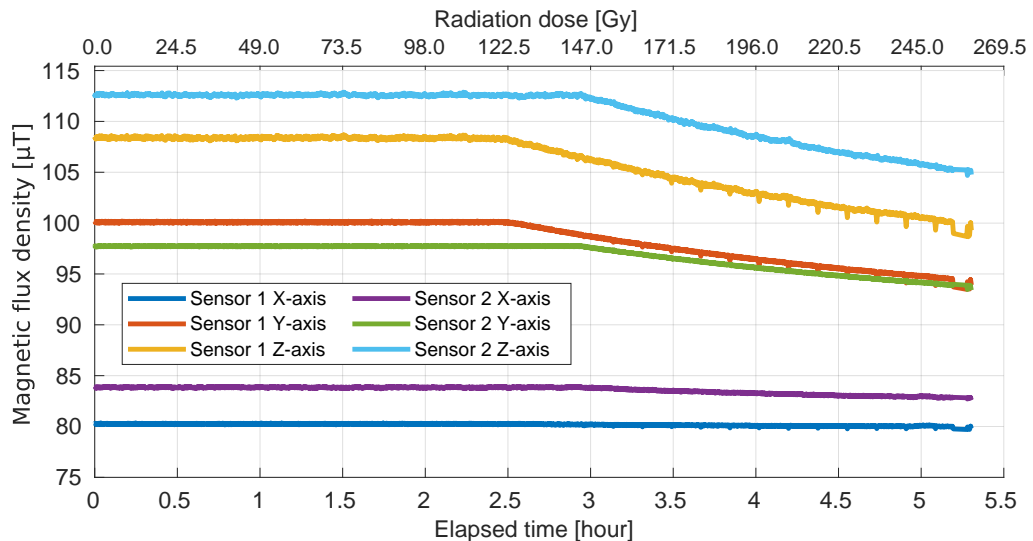


**Figure 7.6.** Magnetic flux density readings of both MMC5983 sensors.

Even the last tested sensor was not spared from the unpleasant consequences of the radiation. Although the MPU6050 has not suffered from the progressive degradation,

its malfunction is visible from the acquired sensor's data shown in figure 7.7. The Y and Z-axis readings have jumped to the sensor's full-scale limits of  $\pm 2[g]$  at about 4.10[hour]. The X-axis reading has also encountered a faulty period later at 4.55[hour], measuring an acceleration close to 0[g]. After one of the following prevention power reset, the sensor has recovered and started to return reasonable data at 4.73[hour]. Reading of the MPU6050's gyroscope seems to have not been affected in any way.

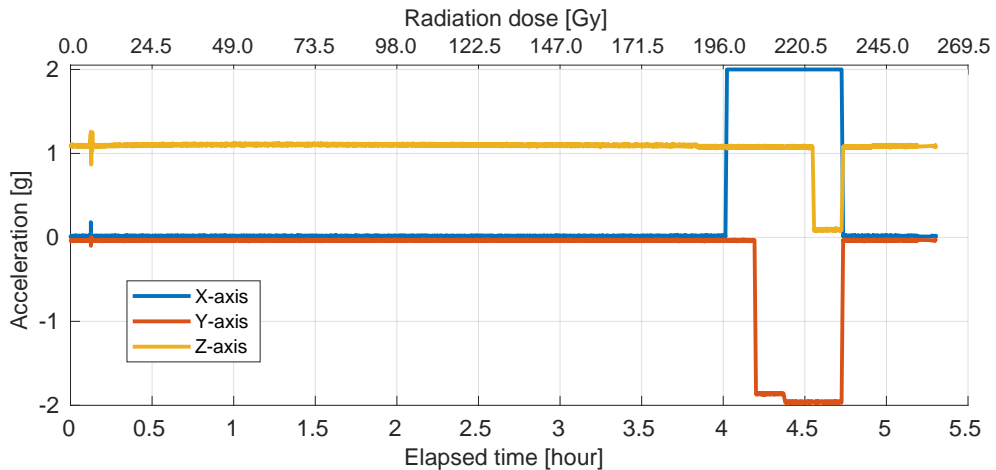


**Figure 7.7.** Acceleration readings of the MPU6050 sensor.

Despite our best effort to record an occurrence of a memory bit-flip inside the Flash memory subsystem, no such event was observed. All three memory ICs were performing normally throughout the entire experiment. Not a single error or malfunction was logged by the OBC. As already stated, a slightly increased temperature was measured by their associated temperature sensor as a sign of their activity (TS1 in figure 7.4).

### 7.2.3 Experiment summary

Unfortunately, we cannot compare the observed performance with the ECSS-Q-ST-60-15C hardness assurance standard [74]. The nominal ionizing radiation dose rate of our experiment has exceeded the upper limit of the required test rate approximately 13.6 times. In other words, the standard requires the test to be conducted at a dose rate of 0.36 - 3.6[Gy/hour], whereas our experiment was carried at 49.0[Gy/hour].

The total ionizing radiation dose sustained by the OBC has exceeded our expectations. The reached total dose of 254.32[Gy] without a single malfunction is comparable to 200 - 300[Gy] certifications of professional OBC manufacturers [26, 30, 28]. However, this radiation testing can serve just as a proof-of-concept. A series of tests aimed at specific subsystems, measuring a variety of voltages and currents, had to be performed to create an accurate image of the OBC's robustness.

# **Chapter 8**

## **Conclusion**

In this thesis, we have contributed to the VST104 project of CubeSat hardware development established by the company VisionSpace Technologies. For this project, we have designed a family of PC/104 format electronics boards, including a universal board, a single onboard computer board, a double redundant onboard computer board, and a FlatSat test bench. We have also managed to properly test out our primary design - the single onboard computer. On top of that, we have successfully conducted its testing under a gamma radiation source and acquired valuable experiment results. In order to provide helpful and accurate documentation of the developed boards, we have included many design details and illustrations into the main body of this thesis.

It is safe to say that our work has already been noticed by the open-source CubeSat community. We have presented our work at an Open Source CubeSat Workshop 2020, igniting a broad discussion about a united PC/104 pinout. At the time of submitting this thesis, an abstract including the VST104 project was accepted for the 5th ESA CubeSat Industry Days. Similarly, another abstract regarding the radiation testing was accepted for the 1st Students Conference on Sensors, Systems and Measurement.

We are also pleased that our work is already being used not only by the VST but also by other organizations. Romanian InSpace Engineering S.R.L. started the development of CubeSat subsystems based on the provided Board Sierra and Element Foxtrot. TU Darmstadt Space Technology e.V. has also received both of these boards for their development purposes. The VST is currently using the VST104 platform for developing their Rust implementation of the telemetry and telecommand packet utilization. Future expansion of our work is planned as VST is interested in integrating a NanoXplore NG-Medium FPGA to the Board Sierra for the development of the POCKET+.

## References

- [1] AGLIETTI, Guglielmo S.. Current Challenges and Opportunities for Space Technologies. *Frontiers in Space Technologies*. 2020. ISSN 2673-5075. Available from DOI 10.3389/frspt.2020.00001.
- [2] CURZI, Giacomo, Dario MODENINI, and Paolo TORTORA. Large Constellations of Small Satellites: A Survey of Near Future Challenges and Missions. *Aerospace*. 2020. ISSN 2226-4310. Available from DOI 10.3390/aerospace7090133.
- [3] GEIB, Filip, José FEITERINHA, and Selman ÖZLEYEN. *An Open-Source on-board computer platform for CubeSats*. Open Source CubeSat Workshop 2020.
- [4] ROTTEVEEL, J., and A.R. BONNEMA. *CubeSat101: Basic Concepts and Processes for First-Time CubeSat Developers*. NASA CubeSat Launch Initiative.
- [5] CDS. CubeSat Design Specification. San Luis Obispo: Cal Poly SLO, 2014. Rev 14.
- [6] REISS, Philipp, Philipp HAGER, Charlotte BEWICK, and Malcolm MACDONALD. New Methodologies for the Thermal Modeling of CubeSats. 2012.
- [7] ROTTEVEEL, J., and A.R. BONNEMA. Thermal control issues for nano and picosatellites. In: *57th International Astronautical Congress*. Available from DOI 10.2514/6.IAC-06-B5.6.07.
- [8] ISRAR, Asif. Vibration and Modal Analysis of Low Earth Orbit Satellite. *Shock and Vibration*. 2014. Available from DOI 10.1155/2014/740102.
- [9] TOORIAN, Armen, Ken DIAZ, and Simon LEE. The CubeSat Approach to Space Access. In: *2008 IEEE Aerospace Conference*. 2008. Available from DOI 10.1109/AERO.2008.4526293.
- [10] PCI/104-Express™ & PCIe/104™ Specification. Including OneBank™ and Adoption on 104™, EPIC™, and EBX™ Form Factors. Los Gatos: PC/104 Consortium, 2015. Rev 3.0.
- [11] NIETO-PEROY, Cristóbal, and M. Reza EMAMI. CubeSat Mission: From Design to Operation. *Applied Sciences*. 2019. ISSN 2076-3417. Available from DOI 10.3390/app9153110.
- [12] LibreCube Board Specification. Paris: European Space Agency, 2019. Rev 1.0. Available from [https://wiki.librecube.org/index.php?title=Libre-Cube\\_Board\\_Specification](https://wiki.librecube.org/index.php?title=Libre-Cube_Board_Specification).
- [13] OSMAN, Duaa A. M., and Sondos W. A. MOHAMED. Hardware and software design of Onboard Computer of ISRASAT1 CubeSat. Available from DOI 10.1109/ICC-CCEE.2017.7867654.
- [14] SANSOE, Claudio, and Maurizio TRANCHERO. Use of FRAM Memories in Spacecrafts. In: 2011. ISBN 978-953-307-456-6. Available from DOI 10.5772/18529.
- [15] SWARTWOUT, Michael. The First One Hundred CubeSats: A Statistical Look. *Journal of Small Satellites*. 2013.

- [16] LANGER, Martin, and Jasper BOUWMEESTER. Reliability of CubeSats – Statistical Data, Developers' Beliefs and the Way Forward. *Proceedings of the AIAA/USU Conference on Small Satellites, SSC16-X-2.* 2016.
- [17] ANGADI, Chetan, Zhora MANJIYANI, Chetan DIXIT, K. VIGNESWARAN, G.S. AVINASH, Prithvi NARENDRA, Shwetha PRASAD, Harish RAMAVARAM, R.M. MAMATHA, G. KARTHIK, H.V. ARPAN, A.H. SHARATH, P. KIRAN, and Visweswaran KARUNANITHI. STUDSAT: India's first student Pico-satellite project. 2011. Available from DOI 10.1109/AERO.2011.5747469.
- [18] JOYA, R. Libertad 1, primer satélite colombiano en el espacio. *Innovaci'on y Ciencia.* 2007.
- [19] SPRINGMANN, J., Benjamin P. KEMPKE, J. CUTLER, and H. BAHCIVAN. DEVELOPMENT AND INITIAL OPERATIONS OF THE RAX-2 CUBESAT. 2012.
- [20] DP-OBC-0402-QAC-DS-1V00-349. DP-OBC-0402 On Board Computer. Bengaluru: Data Patterns Pvt. Ltd..
- [21] iOBC. ISIS On board computer. Delft: ISIS - Innovative Solutions In Space B.V..
- [22] MIT OBC. Cubesat On-Board Computer. Rome: IMT s.r.l., c2016.
- [23] GOS CUBESAT OBC. ON BOARD COMPUTER. Berlin: German Orbital Systems GmbH.
- [24] CubeSat Kit™ Motherboard (MB). Single Board Computer Motherboard for Harsh Environments. San Francisco: Pumpkin Inc., 2012. Rev E.
- [25] ABACUS\_201702. GAUSS OBC ABACUS 2017. Rome: G.A.U.S.S. Srl, 2017.
- [26] KRYTEN-M3. Command & Data Handling. Uppsala: AAC Clyde Space, 2020.
- [27] ANTELOPE OBC. On-board computer designed to keep your mission safe. Gliwice: KP Labs Sp. z o.o..
- [28] NANOSATPRO. Space Qualified Processor Unit. Ankara: STM Savunma Teknolojileri Mühendislik ve Ticaret A.Ş..
- [29] NanoMind A712D. On-board Computer System for mission critical space application with limited resources. Aalborg: GomSpace A/S.
- [30] NA-SB3C2-G0-R4. SatBus 3C2. Columbia, IL: NanoAvionics, Corp..
- [31] STARCIK, Milenko, Filip GEIB, José FEITERINHA, and Tiago NOGUEIRA. *On-board platform with hardware-accelerated telemetry data compression.* 5th ESA CubeSat Industry Days.
- [32] CERN Open Hardware Licence Version 2 - Strongly Reciprocal. Meyrin: CERN.
- [33] Library Conventions / KiCad EDA. Library maintainer rules & guidelines. Genewa: KiCad, 2021. Ver 3.0.28.
- [34] BOUWMEESTER, Jasper, Martin LANGER, and Eberhard GILL. Survey on the implementation and reliability of CubeSat electrical bus interfaces. *CEAS Space Journal.* Springer, Available from DOI 10.1007/s12567-016-0138-0.
- [35] TRIVEDI, Rakesh, and Usha S MEHTA. A survey of radiation hardening by design (RHDB) techniques for electronic systems for space application. *International Journal of Electronics and Communication Engineering & Technology (IJECET).* 2016.
- [36] HASELOFF, Eilhard. SLYA014A. Latch-Up, ESD, and Other Phenomena. Dallas: Texas Instruments Inc., 2000. Rev May.

- [37] FETAHOVIĆ, Irfan, Milič PEJOVIĆ, and Miloš VUJISIĆ. Radiation Damage in Electronic Memory Devices. *International Journal of Photoenergy*. Hindawi Publishing Corporation, 2013. ISSN 1110-662X. Available from DOI 10.1155/2013/170269.
- [38] CHARTER. Component Technical Committee Charter. USA: Automotive Electronics Council , 2017. Rev G.
- [39] ECSS-Q-ST-70-12C. Space product assurance - Design rules for printed circuit boards. Noordwijk: ESA-ESTEC, 2014. Rev 14 July.
- [40] ECSS-Q-ST-70-60C. Space product assurance - Qualification and procurement of printed circuit boards. Noordwijk: ESA-ESTEC, 2019. Rev 1 March.
- [41] TOMASZ, Szewczyk. *TEC-ED IoD Board Specification*. Paris: European Space Agency, 2019. Rev 1.0.
- [42] STM32L series. Ultra-low-power 32-bit MCUs Releasing your creativity. Geneva: STMicroelectronics, c2019.
- [43] DS11585. Ultra-low-power Arm® Cortex®-M4 32-bit MCU+FPU, 100 DMIPS, up to 1 MB Flash, 320 KB SRAM, USB OTG FS, audio, external SMPS. Geneva: STMicroelectronics, c2021. Rev 13.
- [44] AN4555. Getting started with STM32L4 Series and STM32L4+ Series hardware development. Geneva: STMicroelectronics, c2019. Rev 8.
- [45] AN5067. How to optimize STM32 MCUs internal RC oscillator accuracy. Geneva: STMicroelectronics, c2018. Rev 1.
- [46] APP2154. Microcontroller Clock—Crystal, Resonator, RC Oscillator, or Silicon Oscillator? San Jose: Maxim Integrated, 2003.
- [47] SiT8924B. Automotive AEC-Q100 Oscillator. Santa Clara: SiTime Corporation, 2019. Rev 1.7.
- [48] AN2867. Oscillator design guide for STM8AF/AL/S, STM32 MCUs and MPUs. Geneva: STMicroelectronics, c2020. Rev 13.
- [49] ABS07AIG. Automotive & Industrial Grade 32.768kHz Ceramic Base SMD Crystal. Hidden Creek: Abracon LLC, 2020. Rev 12-11-20.
- [50] TPS25940-Q1. TPS25940xx-Q1 2.7-V to 18-V eFuse with Integrated Short-to-Battery Protection. Dallas: Texas Instruments Inc., 2021. Rev January 2021.
- [51] SLVC571. TPS2594x Design Calculation Tool. Dallas: Texas Instruments Inc., c2021.
- [52] 74LVC1G11-Q100. Single 3-input AND gate. Nijmegen: Nexperia B.V., 2016. Rev 2.
- [53] TPS22965-Q1. TPS22965x-Q1 5.5-V, 4-A, 16-mΩ On-Resistance Load Switch. Dallas: Texas Instruments Inc., 2019. Rev December 2019.
- [54] BUSCH, Stephan. *Robust, Flexible and Efficient Design for Miniature Satellite Systems*. Würzburg: University of Würzburg, Faculty of Mathematics and Computer Science, 2016. Doctoral thesis.
- [55] FAJARDO, Isai, Aleksander A. LIDTKE, Sidi Ahmed BENDOUKHA et al. Design, Implementation, and Operation of a Small Satellite Mission to Explore the Space Weather Effects in LEO. *Aerospace*. 2019, Vol. 6, No. 10. ISSN 2226-4310.
- [56] DGQ2788A. Automotive 125 °C Analog Switch Dual DPDT / Quad SPDT, 0.37 , 338 MHz Bandwidth. Malvern: Vishay Intertechnology, INC., 2021. Rev 01-Jan-2021.

- [57] NGUYEN, D.N., and Farokh IROM. Radiation effects on MRAM. 2007. Available from DOI 10.1109/RADECS.2007.5205554.
- [58] SHEIKHOLESLAMI, A., and P.G. GULAK. A survey of circuit innovations in ferroelectric random-access memories. *Proceedings of the IEEE*. 2000. Available from DOI 10.1109/5.849164.
- [59] 002-00124. S25FL256L/S25FL128L 256-Mb (32-MB)/128-Mb (16-MB), 3.0 V FL-L Flash Memory. Chandler: Microchip Technology Inc., 2018. Rev \*H.
- [60] 001-89166. CY15B102Q 2-Mbit (256K×8) Serial (SPI) Automotive F-RAM. Chandler: Microchip Technology Inc., 2017. Rev \*F.
- [61] SLLSET0C. TCAN1051-Q1 Automotive Fault Protected CAN Transceiver with CAN FD. Dallas: Texas Instruments Inc., 2017. Rev May 2017.
- [62] KISLING, Daniel, Abhi AAREY, and Bhavin KUMAR. SLLA419. How to Design Isolated CAN Systems With Correct Bus Protection. Dallas: Texas Instruments Inc., 2018. Rev Jul.
- [63] SKROPPA, Ole-Kristian, and Scott MONROE. SLLA271. Common Mode Chokes in CAN Networks: Source of Unexpected Transients. Dallas: Texas Instruments Inc., 2008. Rev Jan.
- [64] *The Engineer's Guide to Temperature Sensing*. Dallas: Texas Instruments Inc., 2000. Rev May.
- [65] DS22203C. MCP9804: ±0.25°C Typical Accuracy Digital Temperature Sensor. Chandler: Microchip Technology Inc., 2012. Rev May 2017.
- [66] KASEMSADEH, Ben, Aaron HENG, and Amit ASHAR. SNOA967A. Temperature sensors: PCB guidelines for surface mount devices. Dallas: Texas Instruments Inc., 2019. Rev Jan.
- [67] AN4989. STM32 microcontroller debug toolbox. Geneva: STMicroelectronics, c2021. Rev 3.
- [68] TVS Diode Array (SPA® Diodes). Low Capacitance ESD Protection - SP3012 Series. Chicago: Littelfuse Inc., 2020. Rev JC.10/26/20.
- [69] PMP10737. Reverse Polarity and Overvoltage Protection Reference Design for Automotive Systems. Dallas: Texas Instruments Inc., 2015.
- [70] STUSB4500. Standalone USB PD sink controller with short-to-VBUS protections. Geneva: STMicroelectronics, 2020. Rev 5.
- [71] STEVAL-ISC005V1. Evaluation board for the STUSB4500 USB Power Delivery controller. Geneva: STMicroelectronics, 2018. Rev 1.
- [72] UM2650. The STUSB4500 software programming guide. Geneva: STMicroelectronics, 2020. Rev 2.
- [73] STSW-STUSB003. Managing dynamic input power with the STUSB4500 and the STM32F072RB. Geneva: STMicroelectronics, 2018. Rev 1.
- [74] ECSS-Q-ST-60-15C. Space product assurance - Radiation hardness assurance - EEE components. Noordwijk: ESA-ESTEC, 2012. Rev 1 October.

# Appendix A

## Thesis assignment



### BACHELOR'S THESIS ASSIGNMENT

#### I. Personal and study details

Student's name: **Geib Filip** Personal ID number: **483567**  
Faculty / Institute: **Faculty of Electrical Engineering**  
Department / Institute: **Department of Measurement**  
Study program: **Cybernetics and Robotics**

#### II. Bachelor's thesis details

Bachelor's thesis title in English:

**On-board computer for PC104 format CubeSats**

Bachelor's thesis title in Czech:

**Palubní počítač pro CubeSaty formátu PC104**

Guidelines:

- Design a concept of an STM32 based on-board computer for PC104 frame based CubeSats.
- Implement redundancy for the critical components to improve reliability of the design.
- Construct the device and conduct testing of the whole system, e.g. using a flatsat platform.
- Concentrate on providing detailed and accurate documentation of the system.

Bibliography / sources:

- [1] Anil K. Maini et al.: "Satellite Technology: Principles and Applications", John Wiley & Sons, Incorporated, 2014
- [2] Ahmet Bindal: "Electronics for Embedded Systems", Springer International Publishing, Switzerland 2017
- [3] Report Concerning Space Data System Standards, Mission Operations Services Concept, CCSDS 520.0-G-3, Consultative Committee for Space Data Systems, Washington, DC, USA, 2020
- [4] Dogan Ibrahim: "ARM-Based Microcontroller Projects Using Mbed", Elsevier Science & Technology, 2019

Name and workplace of bachelor's thesis supervisor:

**Ing. Vojtěch Petrucha, Ph.D., 13138**

Name and workplace of second bachelor's thesis supervisor or consultant:

Date of bachelor's thesis assignment: **13.01.2021** Deadline for bachelor thesis submission: \_\_\_\_\_

Assignment valid until:

**by the end of summer semester 2021/2022**

\_\_\_\_\_  
Ing. Vojtěch Petrucha, Ph.D.  
Supervisor's signature

\_\_\_\_\_  
Head of department's signature

\_\_\_\_\_  
prof. Mgr. Petr Páta, Ph.D.  
Dean's signature

#### III. Assignment receipt

The student acknowledges that the bachelor's thesis is an individual work. The student must produce his thesis without the assistance of others, with the exception of provided consultations. Within the bachelor's thesis, the author must state the names of consultants and include a list of references.

\_\_\_\_\_  
Date of assignment receipt

\_\_\_\_\_  
Student's signature

**Figure 8.1.** Assignment of this bachelor's thesis.

## **Appendix B**

### **Glossary**

I <sup>2</sup> C	inter-integrated circuit
ADC	analog-to-digital converter
AEC	Automotive Electronics Council
ARM	advanced RISC machines
BGA	ball grid array
BOM	bill of materials
CAN	controller area network
CCSDS	Consultative Committee for Space Data Systems
COTS	commercial off-the-shelf
CPU	central processing unit
DAC	digital-to-analog converter
DCDC	direct current to direct current
DPDT	double pole double throw
DRC	design rule check
EECSS	European Cooperation for Space Standardization
eFuse	electronic fuse
EMI	electromagnetic interference
ESA	European Space Agency
ESD	electrostatic discharge
FFC	flat flexible cable
FPGA	field-programmable gate array
GND	ground
GPIO	general-purpose input/output pin
HSE	high speed external
IC	integrated circuit
JPL	Jet Propulsion Laboratory
LC	inductor-capacitor
LED	light emitting diode
LSE	low speed external
MCU	microcontroller unit
MEMS	microelectromechanical system
MOSFET	metal–oxide–semiconductor field-effect transistor
NA	not applicable
OBC	on board computer
PCB	printed circuit board
PDCU	power distribution and control unit
PDU	power distribution unit
PLL	phase-locked loop
PWM	pulse width modulation
QFN	quad-flat no-leads
QPI	quad peripheral interface

---

RC	resistor-capacitor
RCS	radio communication subsystem
RTC	real time clock
RTD	resistance temperature detector
Rx/Tx	receive / transmit
SMD	surface mount device
SPI	serial peripheral interface
SPICE	simulation program with integrated circuit emphasis
SSOP	shrink small-outline package
SWD	serial wire debug
SWJ-DP	serial wire JTAG debug port
SWO	serial wire output
SWV	serial wire viewer
THT	through-hole technology
TVS	transient-voltage-suppression
UART	universal asynchronous receiver-transmitter
USB	universal serial bus
USB-C	universal serial bus type C
VST	Vision Space Technologies

# Appendix C

## VST104 pinout

Header H1				Header H2			
	1	2			1	2	
	3	4			3	4	
USER_1_1	5	6	USER_1_2		5	6	USER_2_2
SPI_1_CS2	7	8	USER_1_4		7	8	USER_2_4
SPI_1_CS1	9	10	SPI_1_MOSI		9	10	SPI_2_MOSI
SPI_1_CLK	11	12	SPI_1_MISO		11	12	SPI_2_MISO
UART_1_TX	13	14	UART_1_CTS		13	14	UART_2_CTS
UART_1_RX	15	16	UART_1_RST		15	16	UART_2_RST
UART_RCS_1_TX	17	18	UART_RCS_1_CTS		17	18	UART_RCS_2_CTS
UART_RCS_1_RX	19	20	UART_RCS_1_RST		19	20	UART_RCS_2_RST
I2C_1_SCL	21	22	I2C_1_SDA		21	22	I2C_2_SDA
CAN_1_H	23	24	CAN_1_L		23	24	CAN_2_L
GLO_SYNC	25	26	GLO_FAULT		25	26	SUP_5V
CPU_WD_1	27	28	CPU_WD_2		27	28	SUP_3V3
-	29	30	CPU_MODE		29	30	GND
SUP_3V3_REF	31	32	SUP_5V_REF		31	32	AGND
GND	33	34	GND		33	34	-
GLO_KS_1	35	36	GLO_KS_2		35	36	-
-	37	38	-		37	38	-
USER_3_1	39	40	USER_3_2		39	40	USER_4_2
USER_3_3	41	42	USER_3_4		41	42	USER_4_4
USER_5_1	43	44	USER_5_2		43	44	USER_6_2
USER_5_3	45	46	USER_5_4		45	46	-
	47	48			47	48	USER_6_4
	49	50			49	50	
	51	52			51	52	

**Figure 8.2.** VST104 pinout: assignment of PC/104 header pins used in the VST104 project.  
Legend: red - mandatory, orange - optional, green - user defined, blue - legacy pins.

Signal name	Signal purpose
UART_RCS_	UART used explicitly for the RCS*
GLO_SYNC	clock signal of global synchronization
GLO_FAULT	signal setting a global fault flag
GLO_KS_	standard kill switch signal (active high)
CPU_WD_	watchdog signal for each of the OBCs (CPUs)
CPU_MODE	OBC selection signal used in Board Delta

**Table 8.1.** A brief explanation of selected signals from the VST104 pinout. A more specific definition will be provided by the VST in the future. \*radio communication subsystem

## Appendix D

### Photo documentation

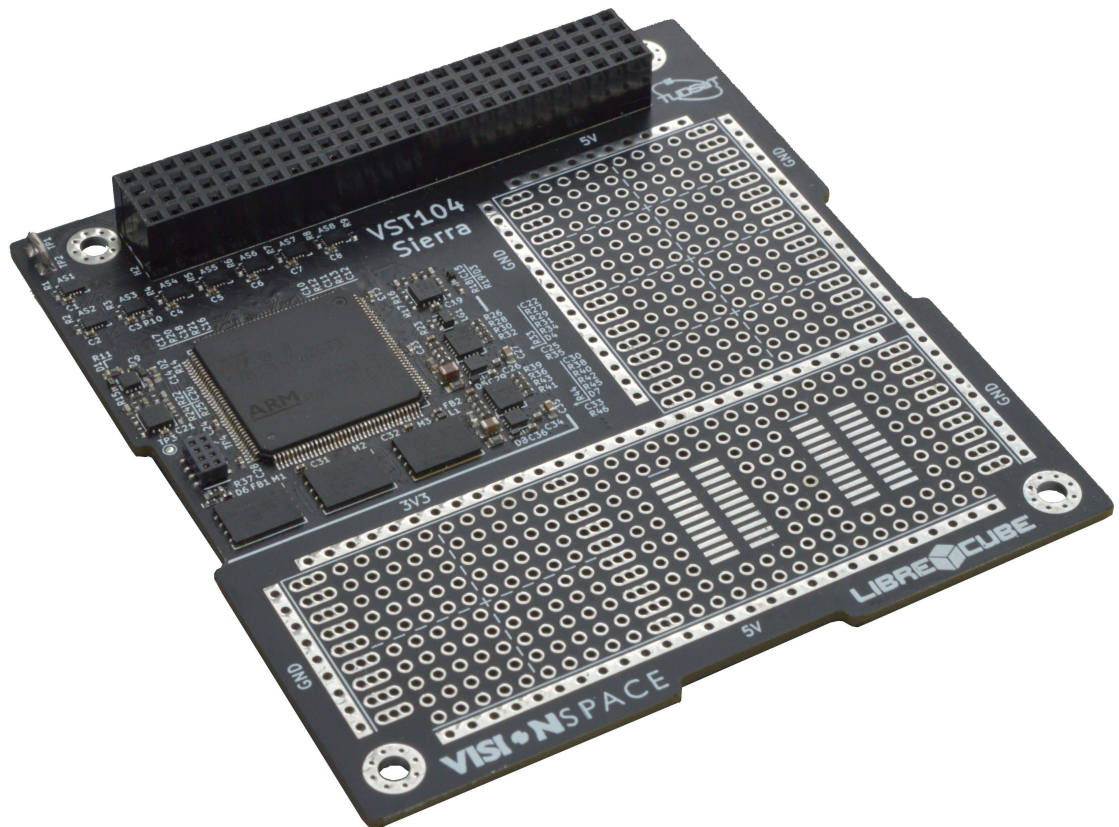
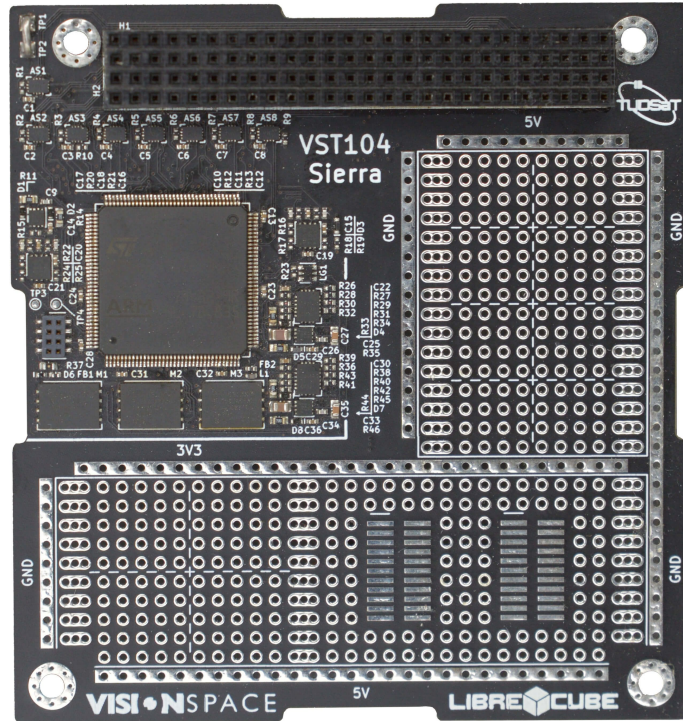
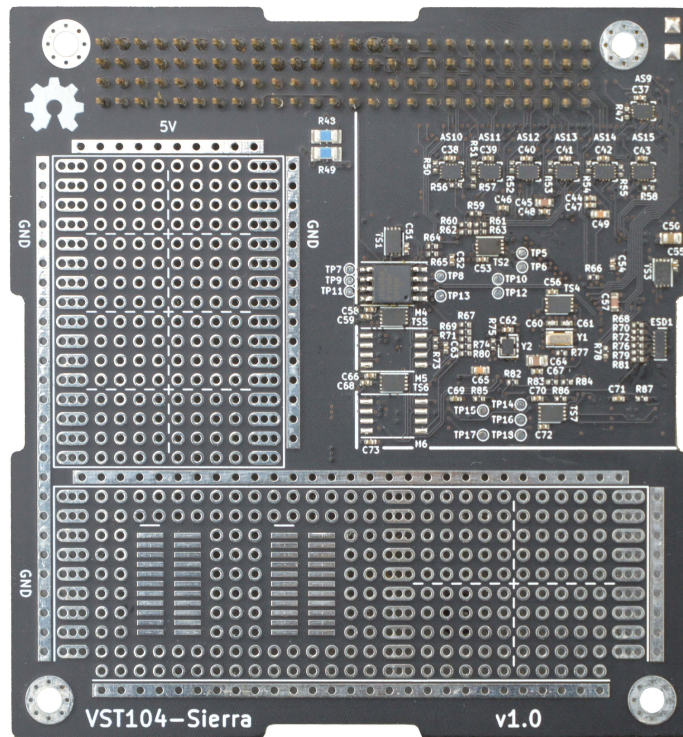


Figure 8.3.



**Figure 8.4.**



**Figure 8.5.**



**Figure 8.6.**

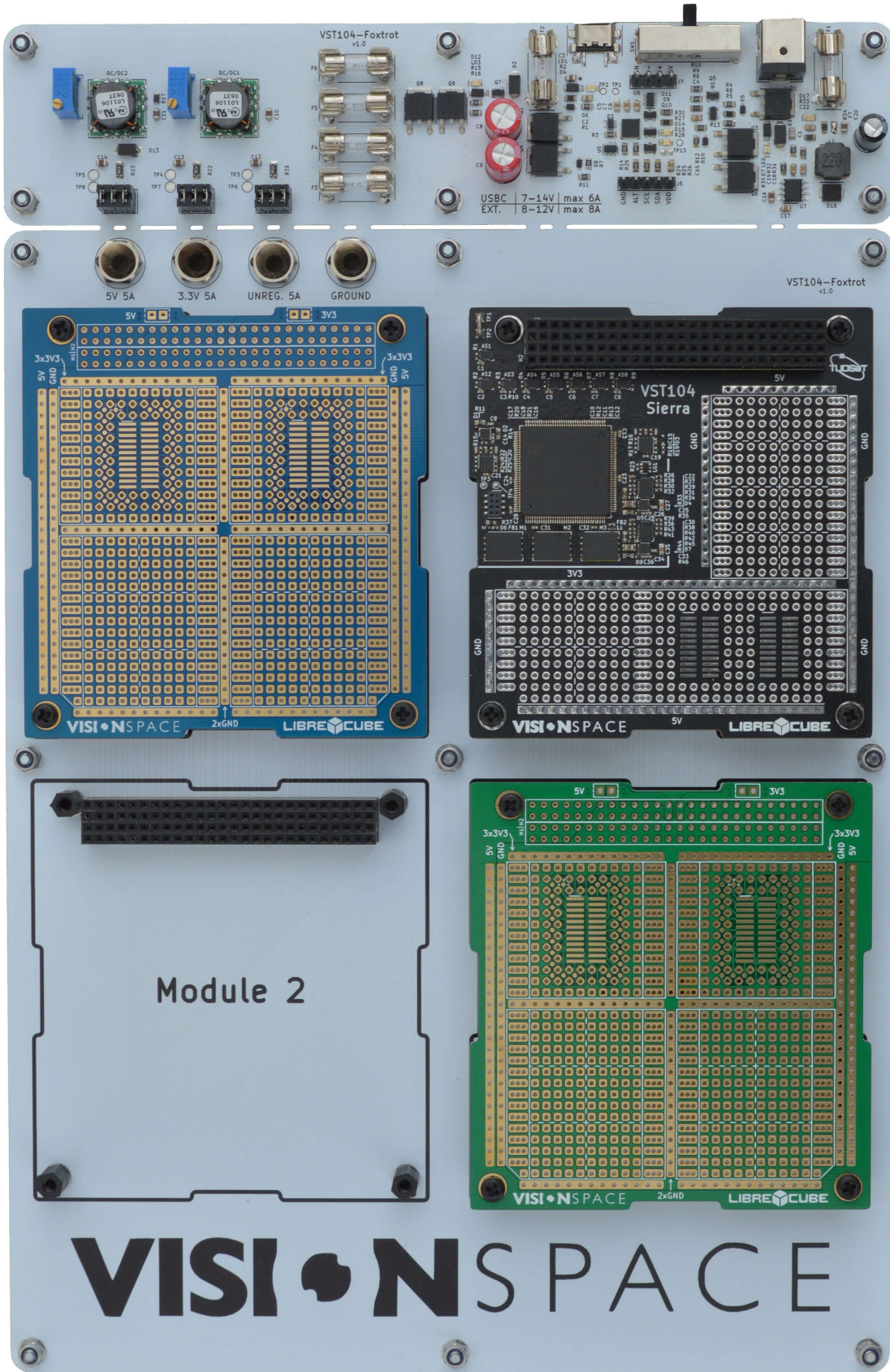


**Figure 8.7.**

## Appendix E

### Over-sized figures

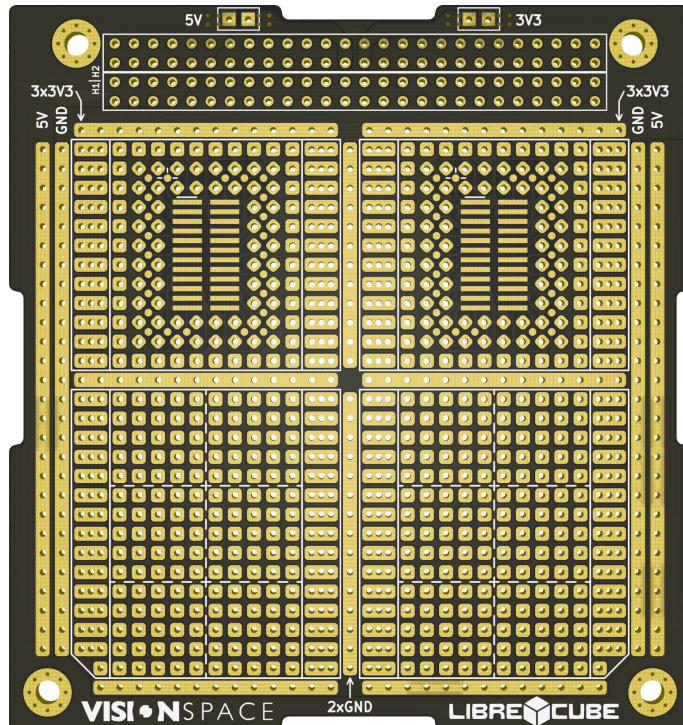


**Figure 8.8.** Visualization of the Board Zero captured from its top side. The dimensions of this 3D render match the actual size of the board 1:1.

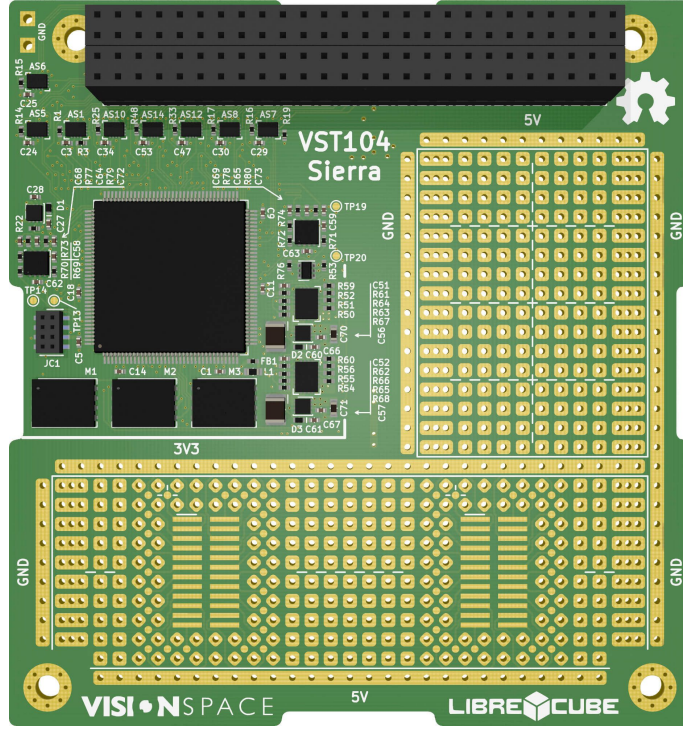


**Figure 8.9.** Visualization of the Board Sierra captured from its top side. The dimensions of this 3D render match the actual size of the board 1:1.

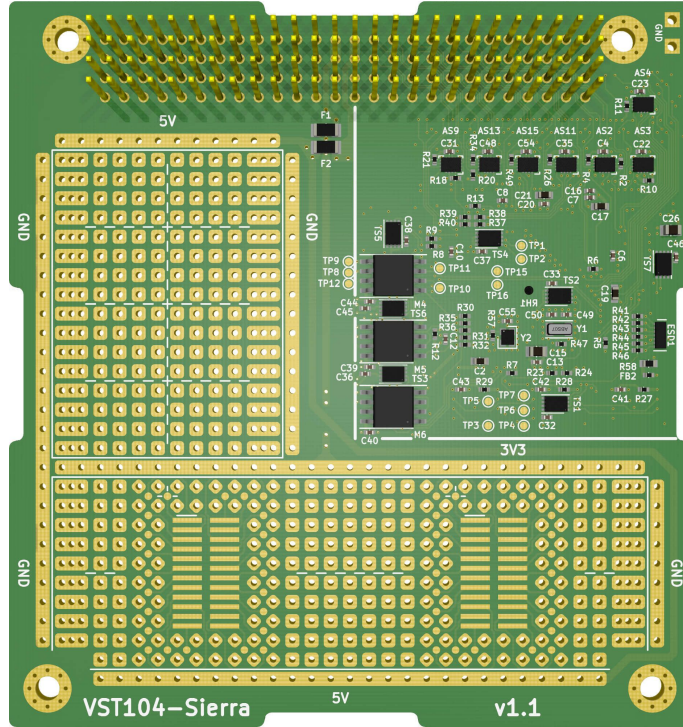


**Figure 8.10.** Visualization of the Board Sierra captured from its bottom side. The dimensions of this 3D render match the actual size of the board 1:1.

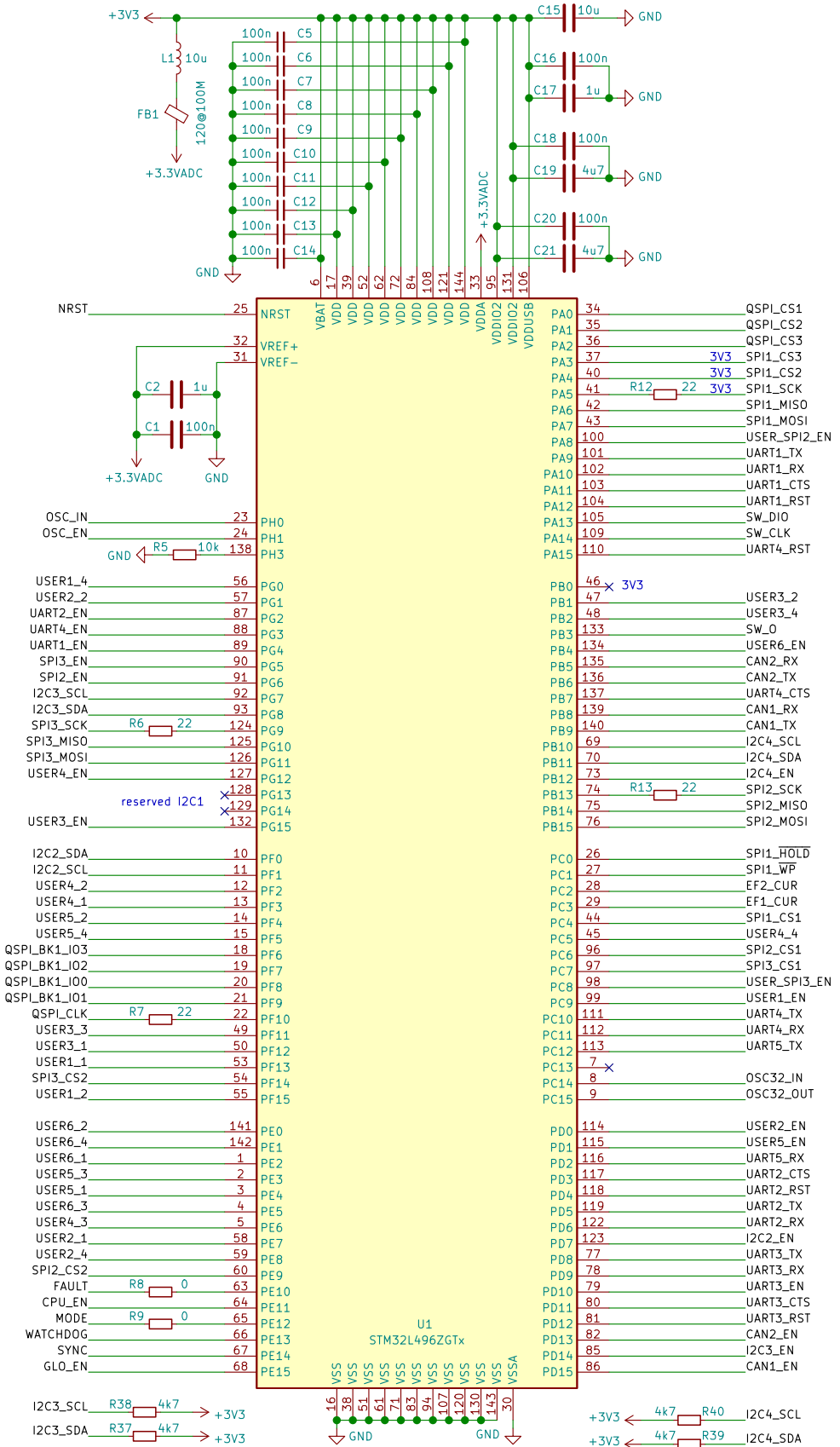


**Figure 8.11.** Schematic diagram of the microcontroller and its auxiliaries.

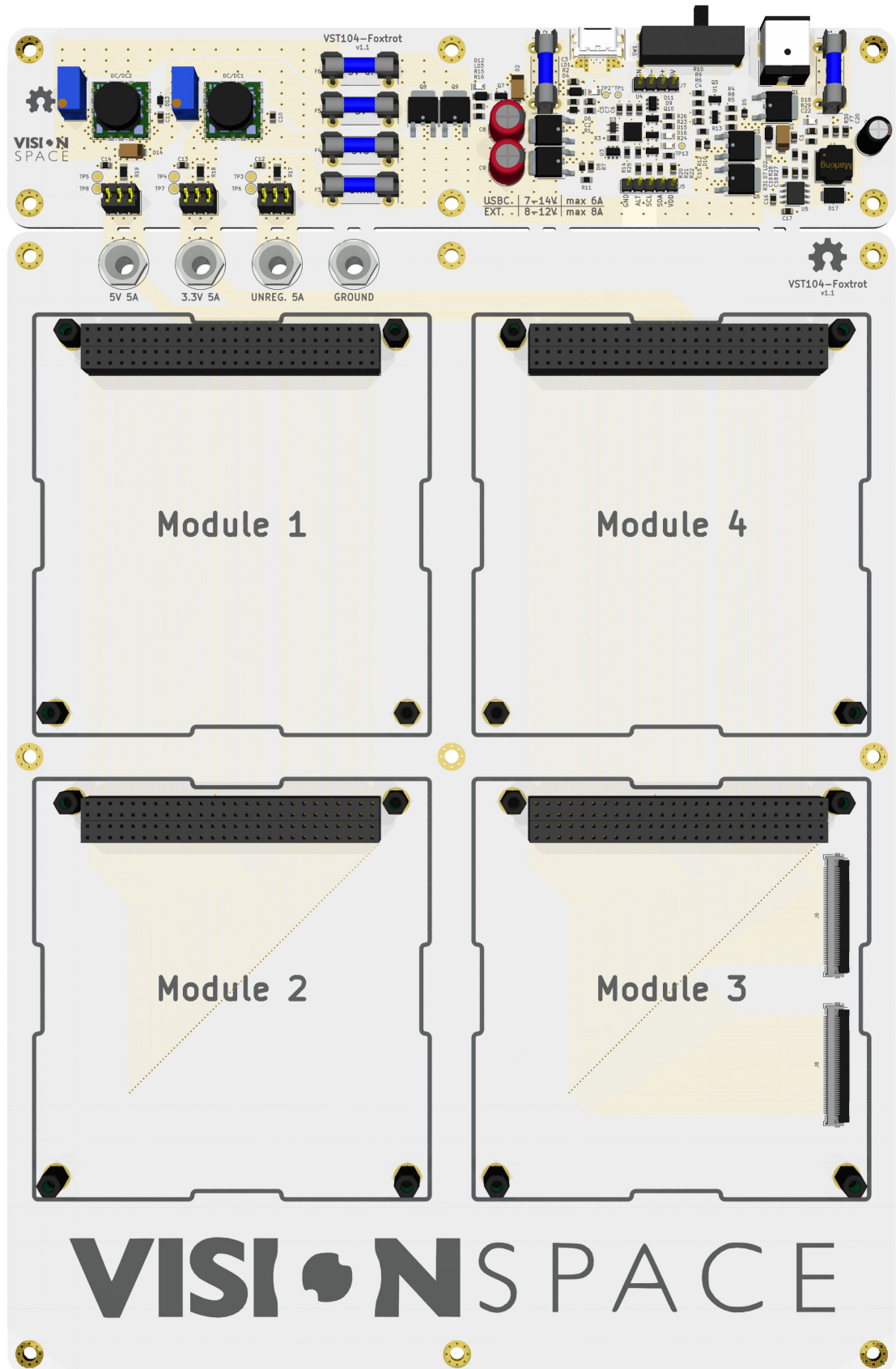


**Figure 8.12.** Visualization of the Element Foxtrot captured from its top side. The dimensions of this 3D render match the actual size of the board 1:1.4.

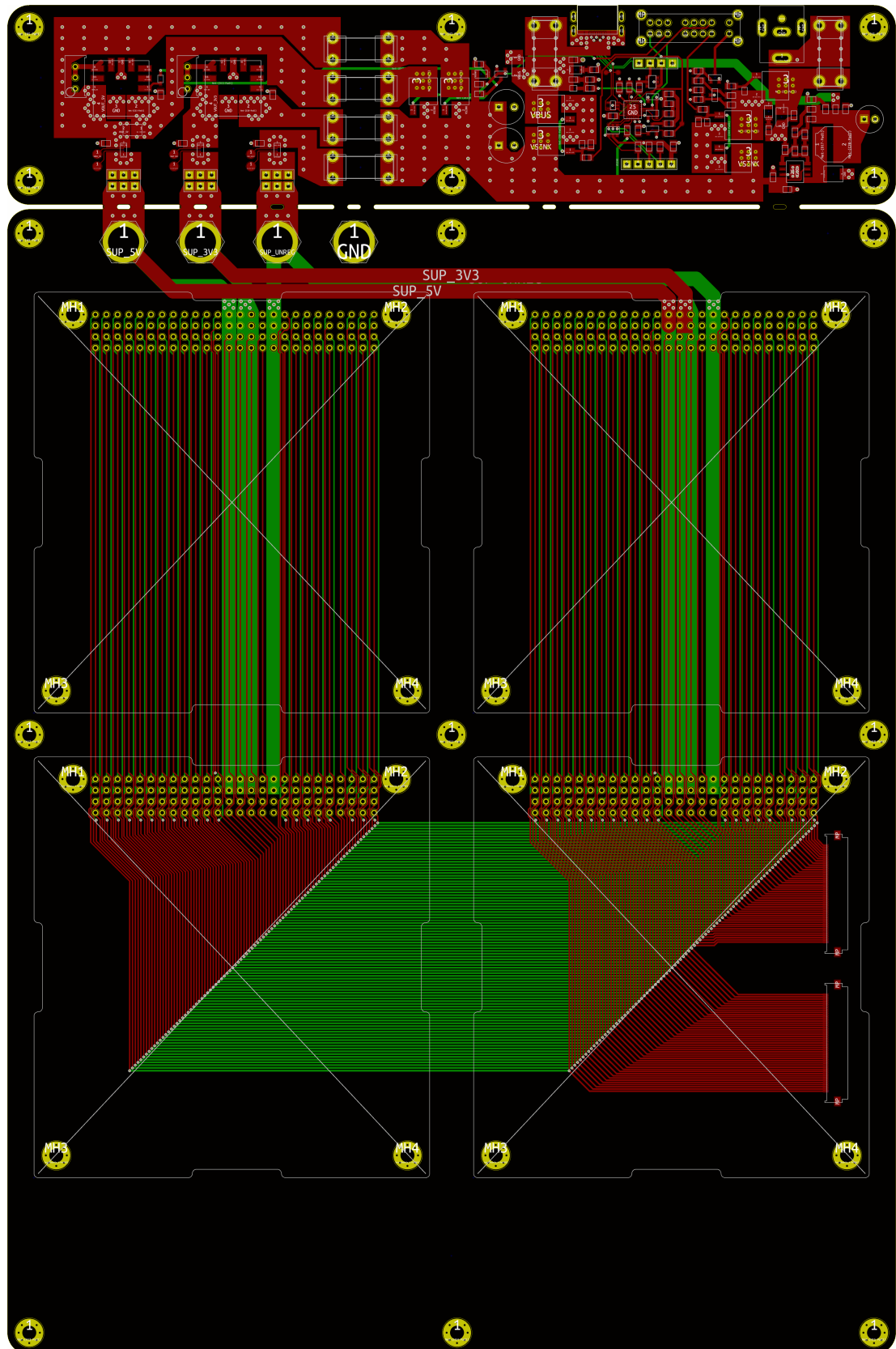


**Figure 8.13.** PCB design of the Element Foxtrot captured directly in the KiCad environment. The dimensions of this render match the actual size of the board 1:1.4.

## Appendix F

### Additional materials

Designator	Power bus [V]	Current consumption [mA]		
		Min.	Typ.	Max.
AS[1-15]	5	-	0.02	0.06
EF[1,2]	3.3, 5	0.14	0.21	0.30
LG1	3.3	-	0.1	4
M[1-3]	3.3	10	25	40
M[4-6]	3.3	-	5	5
TS[1-7]	3.3	-	0.20	0.40
U[2,3]	5	-	40	70
Y2	3.3	-	4.0	4.8

**Table 8.2.** Listing of electronic components power consumption. The values were obtained from the datasheets, and correspond to the normal operation at room temperature.

Designator	Certified part no.	Uncertified part no.	Difference
LG1	74LVC1G11GW-Q100	74LVC1G11GW	auto.
M[1-3]	S25FL256LAGNFI	S25FL256LAGNFI	temp.
	S25FL256LDPNFI	S25FL256LDPNFI	temp., speed
TS[1-7]	MCP9804x-E/MC	MCP9808x-E/MC	accuracy
Q[1-3]	TPS22965W-Q1	TPS22965-Q1 TPS22975	temp. temp., auto.

**Table 8.3.** List of available uncertified variants to some of the OBCs electronic components. Legend: auto. - missing AEC certification, temp. - shrink operational temperature range, speed - decreased frequency, accuracy - decreased accuracy of measurements.